Copyright Warning & Restrictions

The copyright law of the United States (Title 17, United States Code) governs the making of photocopies or other reproductions of copyrighted material.

Under certain conditions specified in the law, libraries and archives are authorized to furnish a photocopy or other reproduction. One of these specified conditions is that the photocopy or reproduction is not to be "used for any purpose other than private study, scholarship, or research." If a, user makes a request for, or later uses, a photocopy or reproduction for purposes in excess of "fair use" that user may be liable for copyright infringement,

This institution reserves the right to refuse to accept a copying order if, in its judgment, fulfillment of the order would involve violation of copyright law.

Please Note: The author retains the copyright while the New Jersey Institute of Technology reserves the right to distribute this thesis or dissertation

Printing note: If you do not wish to print this page, then select "Pages from: first page # to: last page #" on the print dialog screen

Behavior of Tee-shaped Reinforced Concrete Columns Subjected to Biaxial Bending and Axial Compression

By

Antoun Romanos Nader

Thesis submitted to the faculty of the Graduate School of the New Jersey Institute of Technology in partial fulfillment of the requirements for the degree of Master of Science in Civil Engineering
1984

APPROVAL SHEET

Title of Thesis : Behavior of T-shaped Reinforced Concrete Columns subjected to Biaxial Bending and Axial Compression

Name of Candidate : Antoun Nader
Master of Science in Civil Engineering

Thesis and Abstract Approved:

C.T. Thomas Hsu
Associate Professor,
Department of Civil
and Environmental
Engineering

July 5, 1984
Date

Signatures of other members of the thesis committee :

June 6, 1984
Date

7/3/84
Date

VITA

Name: Nader, Antoun.

Degree and date to be conferred: MSCE, I984.

Secondary education: Al-Carmelia school, Tripoli, Lebanon, June I978.

Collegiate institutions attended	Dates	Degree	Date of Degree
New Jersey Institute of Technology, Newark, N.J., U.S.A.	9/80-I0/82	Bachelor of Science in Civil Engineering	Oct.I982
New Jersey Institute of Technology, Newark, N.J., U.S.A.	9/82-5/84	Master of Science in Civil Engineering	May.I984

Major: Civil Engineering.

Title of Thesis : Behavior of Tee-shaped Reinforced Concrete Columns Subjected to Biaxial Bending and Axial Compression

Antoun Nader : Master of Science, I984

Thesis directed by: Prof: C.T. Thomas Hsu

Abstract

The investigation deals with the effect of eccentric loading on the moment-curvature relationship of reinforced concrete tee columns.

The test program consisted of two series of tee-shaped reinforced concrete columns, loaded biaxially at constant angle from the principle axes. Their end conditions were assumed to be pinned-ended.

Loads, at constant rate, were gradually applied until failure. At each loading stage, measurements were made for the strains and deflections at the mid span section.

The experimental and theoretical results of the load-deformation and moment-curvature were compared and found that the analytical approach proposed by Hsu is applicable to irregular sections such as tee columns, under small and large eccentricities, but tended to underestimate slightly the axial load and the moment-curvatures at failure.

To my wife

and

my parents

Acknowledgements

The author is indebted to professor C.T. Thomas Hsu for his valuable aid, assistance, direction and guidance of the work necessary to prepare this thesis.

I thank Mr. Jimmy Chen whose constructive comments and observations were extremely helpful.

The author wishes to express his appreciation and gratitude to graduate students, Messrs. J. Tarabay, S. Yalamurthy and A. Shah, who assisted him in casting specimens and conducting tests.

I also thank Messrs. E. Skurbe and D. Diserio, who operated the testing machine during the tests.

I also thank Monica Yoma who assisted in typing this thesis.

Table of Contents

List of Figures

List of Tables

List of Notations

Ak = area of element k

ε_s = strain in tension of steel

e_x = eccentricity along x-axis

e_y = eccentricity along y-axis

ε_c = compressive strain in concrete at the extreme fibre

ε_k = strain across the element k

ε_p = uniform strain due to an axial load P

Es = modulus of elasticity of tension steel

ε_u = ultimate concrete compressive strain

f'c = maximum concrete compressive stress

fy = yield strength of steel reinforcement

k = element number

kd = distance between Ec and the point of zero strain

l = total length of the column

l' = length of the column with respect to the ends of the prismatic shaft along x and y axis

Mx = bending moment about x-axis

My = bending moment about y-axis

P = axial load (compression)

P_3 = the maximum axial load calculated considering the effect of the mid-height deflection components δ_{zx} and δ_{zy}

S = spacing of lateral reinforcement

Xk = the position of the centroid of element k along x-axis

Yk = the position of the centroid of element k along y-axis

ϕ_x = the curvature produced by the bending moment component Mx and is considered positive when it causes compressive strains in the positive y direction

ϕ_y = the curvature produced by the bending moment component My and is considered positive when it causes compressive strains in the positive x direction

$\hat{\delta}_x$ = actual deflection at mid-height along x-axis

$\hat{\delta}_y$ = actual deflection at mid-height along y-axis

$\hat{\delta}_{2x}$ = theoretical deflection at mid-height along x-axis

$\hat{\delta}_{2y}$ = theoretical deflection at mid-height along y-axis

= reinforcement index

Chapter I

General introduction and scope of research

A. Introduction

Next to rectangular and circular shapes, irregular sections of reinforced concrete columns may be encountered in modern building designs since they can be used at outside, reentrant building corners, perimeter and core walls. Due to the locations of the columns, the shapes of the buildings and the nature of the applied loads, these columns may be designed to carry axial load combined with biaxial bending. Nevertheless, information for their analysis and design is not generally available to structural engineers, either in working stress, ultimate strength and limit design methods.

This investigation reported in this paper deals with the effect of axial load and biaxial bending on the moment-curvature and load-deformation relationships of reinforced concrete tee columns.

The purpose of this investigation is to obtain information regarding the general behaviour of load-deflection and moment-curvature of biaxially loaded short tee columns, as the applied load is increased monotonically from zero until failure, furthermore, the experimental results are compared with the computer analysis values to assess the accuracy of the computer program and to recommend whether the analytical approach developed by Hsu is applicable to

irregular sections under small and large eccentricities.

Finally, a knowledge of the deformation capacity of a reinforced concrete column is important in reinforced concrete design. The ability of a structure to resist earthquake motions or blast loading is a function of both the strength and the deformation capacity of its columns. This information is also needed if limit design methods are to be used.

B. Current analysis and design methods

The investigation or design of a regular and irregular section subjected to an axial compression in combination with bending moments about both principal axes has received considerable attention. Three approaches have been suggested and are either based on the assumption that the failure at a section occurs when the equilibrium equation and strain compatibility equations are violated or when the maximum concrete strain exceeds a certain predefined value.

The first approach is based on the ultimate strength theories which are considered simple and sufficiently accurate for practical purposes. The failure is defined in terms of a limiting strain or stress in the concrete and the reinforcing steel. Also the stress distribution in the compression zone of a section is defined in terms of the stress block parameters which are determined experimentally and may not be applicable to other than the test conditions. This approach did not take into account the properties of a section, its shape, the amount of steel reinforcement, the rate of loading and the lateral reinforcement.

The second approach is based on the maximum concrete strain. The failure is defined when the strain in the extreme compression fibre reaches a certain value, ε_u. The numerical approach in this group is based on the equations

of equilibrium and strain compatibility at a section and the given stress-strain curves for the concrete and the reinforcing steel. The selection of the extreme concrete compression strain ε_c or tensile strain ε_s as a trail value will determine the position of the neutral axis, bending moment and curvature after few iterations.

The main difference between ultimate strength theories and the second group is that the latter uses generalized stress-strain curves and functional failure criterion. The effect of loading rate, lateral reinforcement etc. can be taken into account by the adoption of a general stress-strain relationship for concrete. Failure or ultimate strength is defined as the loading condition at which a section reaches its maximum capacity.

The third approach is based on maximum concrete and steel strains. Investigations in this group modified the extended Newton-Raphson method or method of successive approximation to determine the strain and curvature distributions of a reinforced concrete section. The failure is defined as if the maximum strains in the concrete or the steel reinforcement exceed certain predefined maximum values, the section is considered to have failed.

C. Previous work

A number of papers have been written which give procedures based on fundamental strength of materials techniques for calculating the capacity of concrete columns subject to biaxial bending. The trial and error method was published by the following investigators, among them:

H. Craemer presented an iterative method of calculating the capacity of members subjected to stress bending. The effects of axial load and of compression force are also presented.[4]

Tung Au gave a similar presentation of members subject to skew bending and presents design charts to simplify the solution of the many equations and conditions involved.[1]

K.H Chu and A. Pabarcius gave a quite rigorous and completely general presentation of a procedure to calculate biaxial bending capacity. It is even applicable to cross-sections of arbitrary shape.[13]

Fleming and Werner gave a design procedure which is based on the existence of a set of design curves for each concrete section. The design curves are basically equivalent to a three dimensional interaction surface for each column.[7]

Recently published methods are based on the concept of failure surfaces in columns. Notable among them are the contributions of the following investigators:

Furlong investigated many columns and plotted their capacity as contours of moment about two axes to give insights into the behavior of biaxially loaded columns. He described the variations of the moment capacities from the circular curve for different axial loads and for different percentages of reinforcement (from 1% to 4%). Also of particular interest for small eccentricities about one of the axes, that the moment capacity about the other axis remains virtually constant.[10]

Pannell presents a method of calculating the biaxial capacity based on the uniaxial capacities. It requires the use of charts and the use of a trigonometric interpolation formula.[17]

Boris Bresler suggests two methods, one the equation $\frac{1}{Pi} = \frac{1}{Px} + \frac{1}{Py} - \frac{1}{Po}$ which is exact for elastic materials but is merely an approximation for reinforced concrete columns. The equation has been used frequently and gives reasonable results for loads above balance condition load, but it is of questionable accuracy for loads less than balance.

The equation $\left(\frac{Mnx}{Mox}\right)^n + \left(\frac{Mny}{Moy}\right)^n = 1$ has been shown that no single value can be assigned to the exponent n to represent the true shape of the load contour in all cases.[3]

Meek showed that the relationship between moment about two axes can be represented by two straight lines. The scatter of his tests results indicate that the two straight lines may

actually be just as accurate a representation of column capacity as the curve calculated by exact procedures. Any error introduced by this assumption is on the conservative side.

The following investigators published some methods based on maximum concrete and steel strains , among them:

Cranston suggested a numerical method in which biaxial moment curvature relationships under constant axial force can be obtained from zero load to the maximum moment capacity. He realized that difficulties arose in the handling of a strain softening material when a large part of a cross section has negative stiffness.[5]

Farah and Huggins solved the simultaneous non-linear equations by Newton-Raphson method in their computer program and concluded that their approach can determine the column deflected shape for various axial load values. Also this information can be used to determine the buckling load in the case of a short column.[6]

Hsu developed a numerical method for determination of strain and curvature distributions in reinforced concrete columns subjected to biaxial bending. The method has the ability to use any standard reinforced concrete section geometry and material properties. The program gives the information for the stress and strain distributions across the section, the ultimate strength and interaction surface of biaxially loaded

short columns, also approximate the rotation and the deflection for reinforced concrete pinned-ended short columns.[13]

Chapter II

Experimental program

A. Description of test specimens

A total of six tee columns were tested under combined axial load and biaxial bending. This adds significantly to the available test results. All columns were of the same size, shape, materials and reinforcement details. The details of geometry for these specimens are shown in figure 2-1 and table 2-1.

The specimens were divided into two series, each series comprising three identical columns, were tested at different angles measured from the principal axis. Two loading brackets were provided at each column end to assist with the application of biaxially eccentric loads. The brackets were designed heavily to prevent any premature failure. Each column was reinforced with eighteen #3 bars, grade 60 or 75, held together by ties #1 mild steel bars at two inch centers at the brackets and at three inch centers throughout the length of the column. The ties were connected to the main reinforcement by binding wires.

In both series, each specimen was tested under axial load and biaxial bending in order to determine the ultimate moment and curvature as well as the full moment-curvature relationship of the column. In each of these tests the axial load was gradually applied until failure. Strains at the midspan cross section were measured on a six inch gauge length

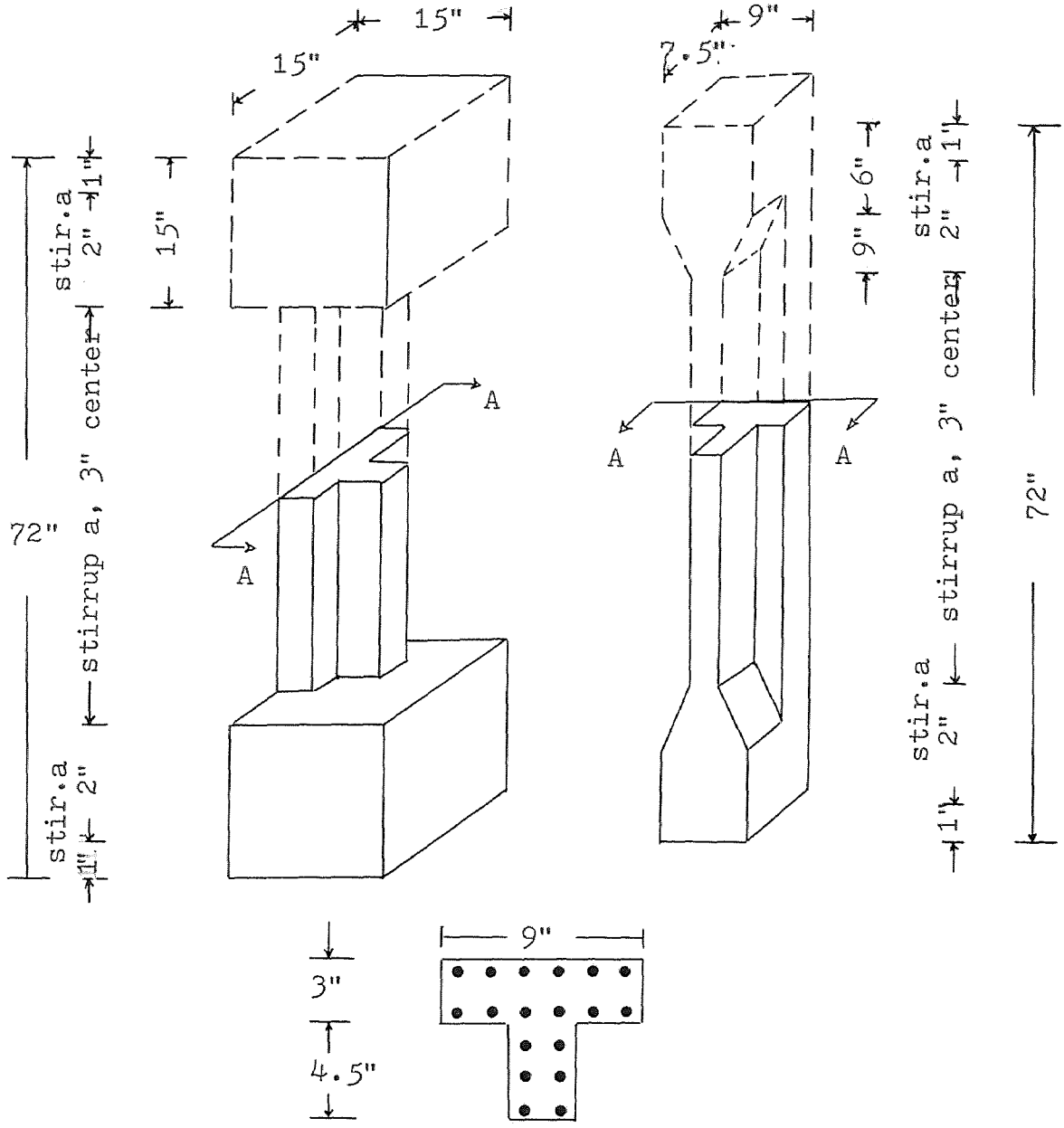

Section A-A

Figure 2-1 Specimen details for both series

Table 2-1 Physical characteristics of columns tested

Specimen	No. and size of bars	percent	f'c (psi)	fy (ksi)	$E_s x 10^6$ (psi)	ex (in)	ey (in)	l (in)	l' (in)	S (in)
T-1	18-#3	4.88	4250	75.5	31.0	2.37	2.50	72	42	3
T-2	18-#3	4.88	4250	65.0	30.5	7.44	1.50	72	42	3
T-3	18-#3	4.88	4250	75.5	31.0	2.09	2.18	72	42	3
T-4	18-#3	4.88	5850	75.5	31.0	2.31	2.37	72	42	3
T-5	18-#3	4.88	4850	65.0	30.5	5.80	1.12	72	42	3
T-6	18-#3	4.88	4850	75.5	31.0	3.00	0.56	72	42	3

by means of Demec mechanical gauge, deflections were measured at midspan of the column with Ames dial gauges. The 3"x6" concrete cylinders were tested in compression until failure and the ultimate compressive loads were recorded.

B. Fabrication and materials

The concrete used for casting the test specimen was prepared from a graded mixture of crushed quartz sand, Portland cement type III and water. Coarse aggregate was used in specimen T-4 only. The mix details are presented in table 2-2.

The specimens were cast in a horizontal position in 5/8" thick plywood reusable formwork. The form was built in sections and assembled together by means of screws to ensure the removal of the test specimen with ease and within short period of time. The form was adequately braced by 2"x 4" lumber in order not to allow the concrete to bulge outward due to its pressure. The interior surfaces of form were coated with a thin layer of oil to deter adhesion between the fresh concrete and the form surfaces. Chairs were used to provide the required cover between the steel and the form surfaces. Reinforcement was assembled into a unit before it was placed into the form. Concrete was mixed by power driven mixer with capacity 16 cubic feet. Mixing time for each batch was approximately five minutes. After the concrete was placed by layers into the formwork, high frequency vibrator was used to compact and facilitate the concrete flow around the closely spaced reinforcement.

Three batches of concrete were used in casting the specimens. Specimens T-1 to T-3 were in the first batch, T-5 and T-6 the second batch and T-4 the final batch. For each batch

Table 2-2 Mix details

Column	Portland cement	Mix proportion c: s: g	w/c ratio	f'c (psi)
T-1	Type III	1:3	0.66	4250
T-2	Type III	1:3	0.66	4250
T-3	Type III	1:3	0.66	4250
T-4	Type III	1:2.3:4.3	0.60	5850
T-5	Type III	1:3	0.60	4850
T-6	Type III	1:3	0.60	4850

three 3"x 6" test cylinders were cast. One cylinder was taken from the concrete used at the begining, the middle and the end of each cast.

The test specimen and the control cylinders surfaces were covered with wet burlap for seven days and later kept in storage until they were tested at the age of 14 days. The cylinders were loaded to failure to determine the concrete compressive strength.

A tension test was performed on a small sample of bars to obtain the mechanical properties. The stress-strain curves for both grades are shown in figure 2-2 and 2-3 respectively.

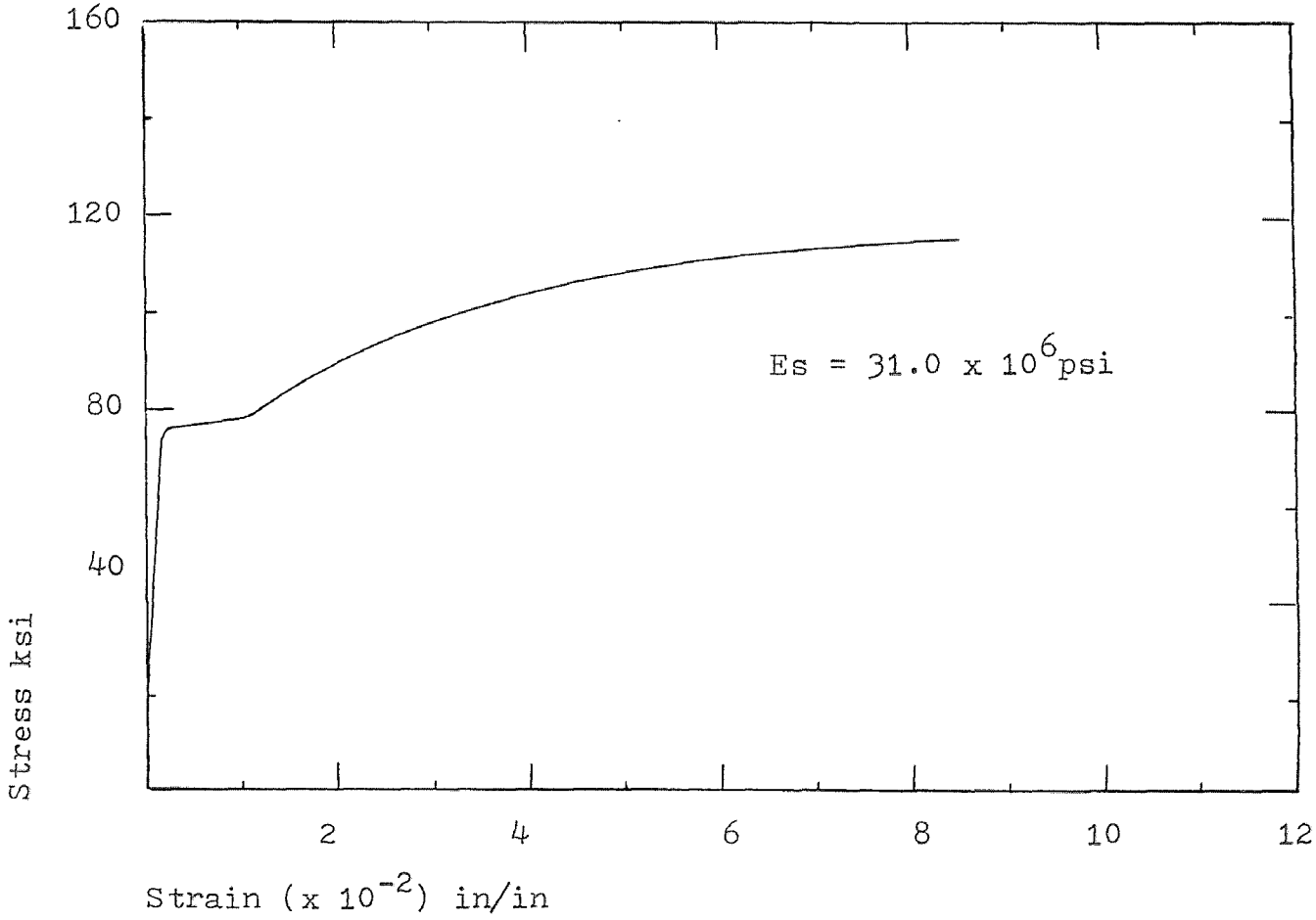

Figure 2-2 Experimental steel stress-strain curve for specimen T-1, T-3, T-4 and T-6

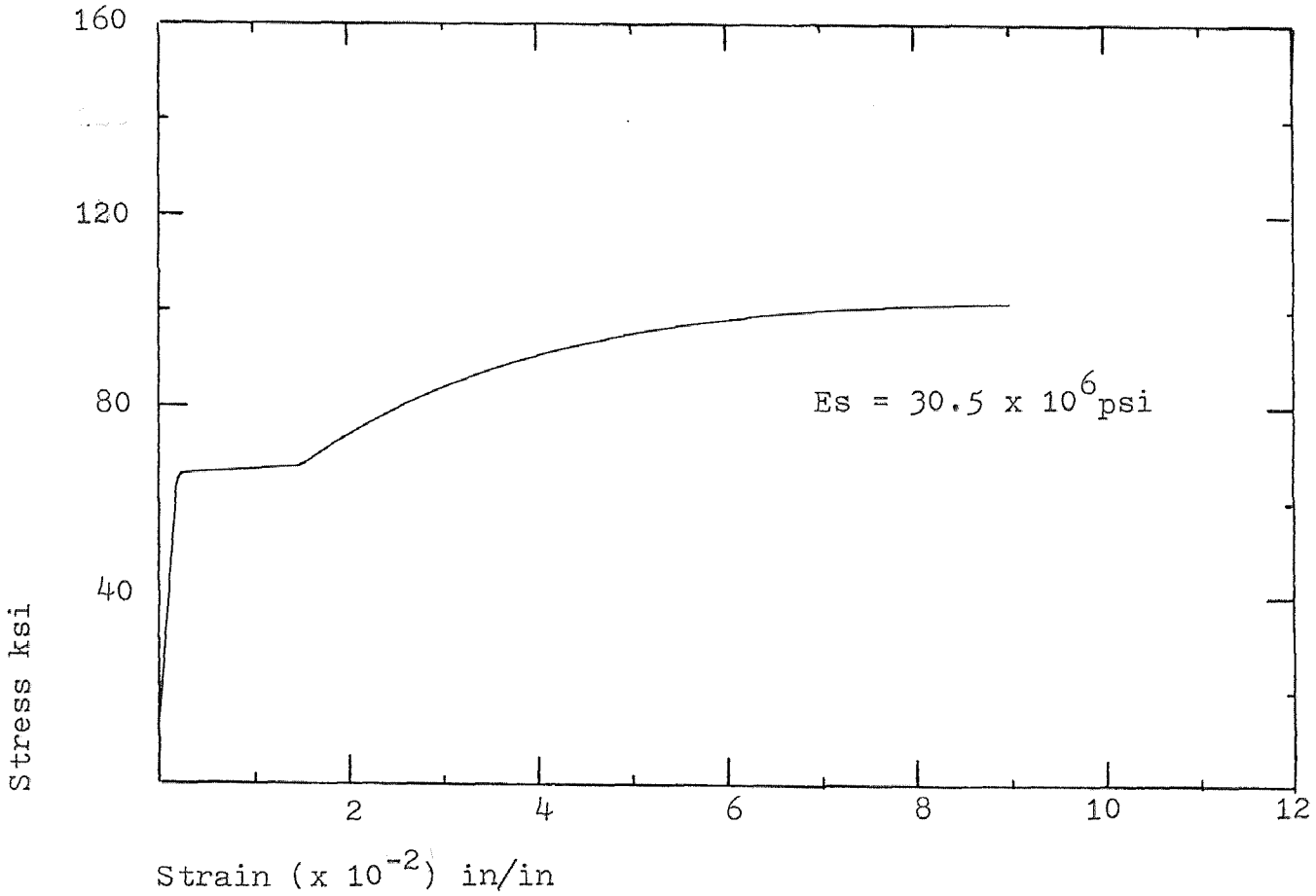

Figure 2-3 Experimental steel stress-strain curve for specimen T-2 and T-5

C. Instrumentation

The required measurements in the investigation for biaxially loaded columns are strains and deflections. Each specimen was fully instrumented with Demec and Ames dial gauges on the column midspan section. Two types of deformation data were recorded:

1. Lateral deflections at column midspan.
2. Longitudinal concrete strains on the tension and compression faces of the column midsection.

Lateral deflections were measured by means of a dial extensometer (range = 2-in, least count = 0.001-in) mounted on a rigid rod.

The instrument used to measure the strain values between two Demec points is the 6-in range Demec mechanical gauge with a least count of 0.0001-in. In addition to the deformation data, readings from the axial load were also recorded. As failure appeared to be imminent all instruments were removed due to sudden failure and possible harm to instrumentation. A hydraulic pressure transducers with a 100 ton capacity were used to control the actual application of the axial loads. Excellent load control was achieved.

D. Column test

All columns were tested in a horizontal position as shown in figure 2-4 and 2-5 respectively. Each test specimen was carefully adjusted so that the load points marked at both end faces will coincide with the hydraulic ram center at one end, the swivel head on the other. Prior to emplacement of the pins, a smooth, level bearing surface of high strength steel plate was used to cover each end of the column. An initial load was applied to the column to keep the pins and plates in position. At each stage of loading, surface strains in concrete and the deflections of the column about the principal axes were recorded. Measurements at each interval lasted for about five minutes. Readings were taken at increments of 500 psi for small eccentricities and 250psi for large eccentricities. Observed data were recorded as the experiment progressed. When crushing or instability became likely, all instruments were removed and failure load was applied and recorded. Each test duration, excluding the specimen set up, lasted for about two hours.

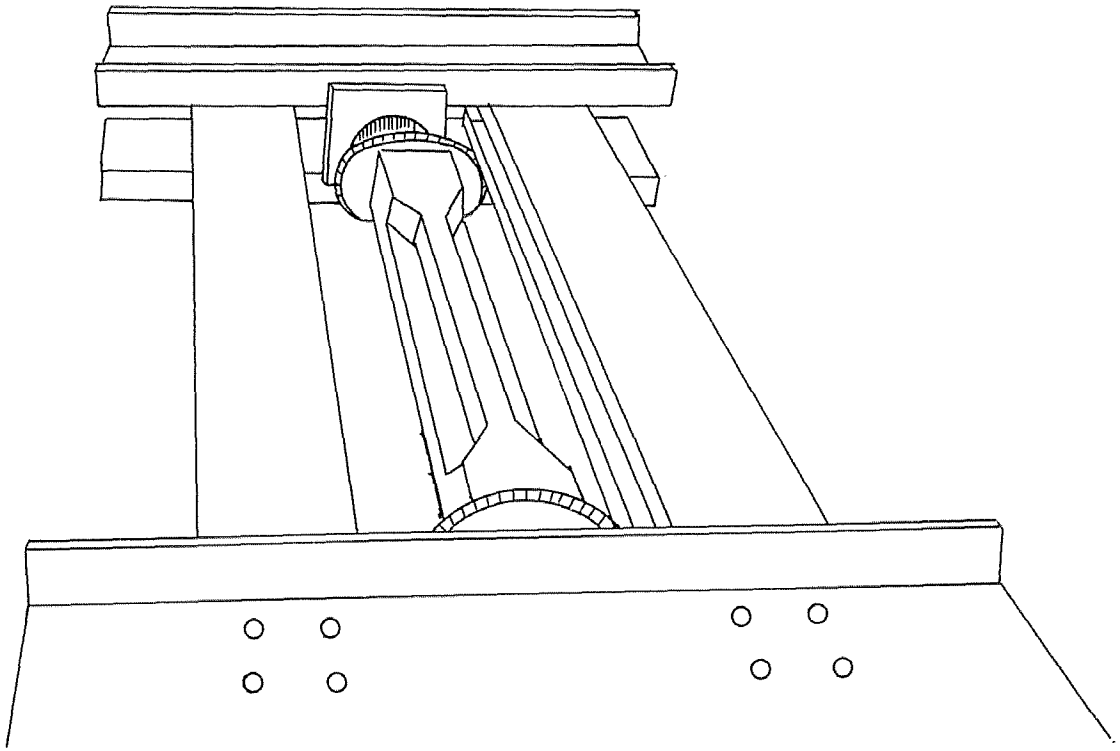

Figure 2-4 Loading arrangement in columns with small eccentricities

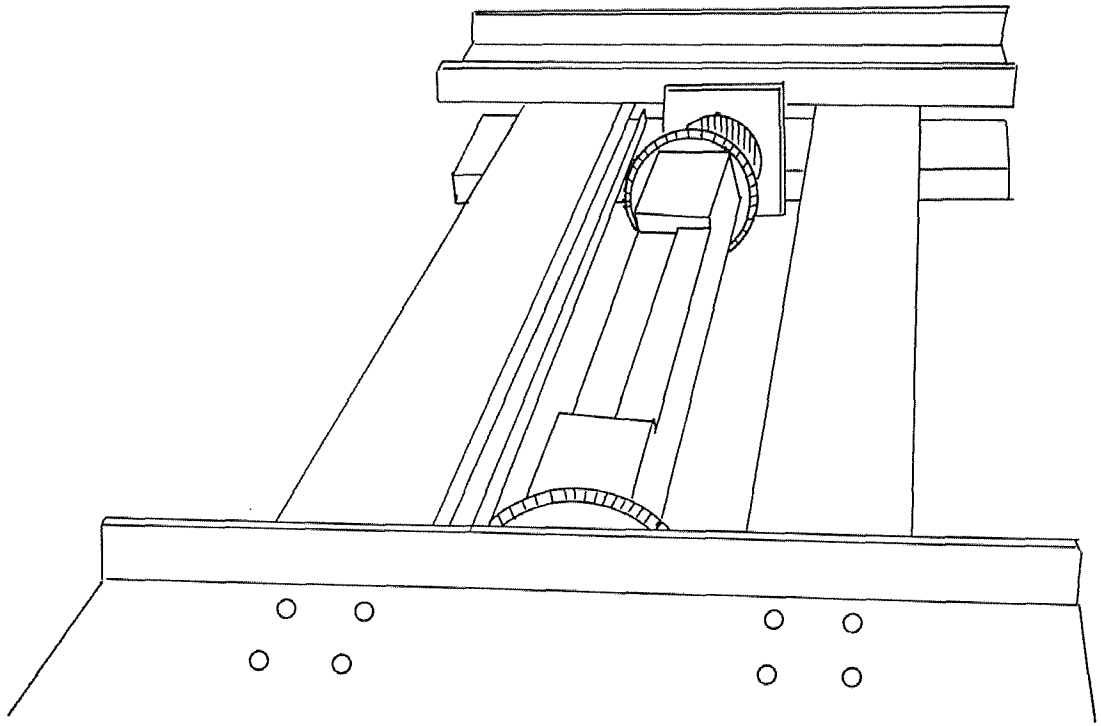

Figure 2-5 Loading arrangement in columns with large eccentricities

E. Specimen failure

At the initial loading stage, cracks were not visible to the naked eye. The development of cracks increased slowly as the load increased presumably due to the small but nevertheless existing tensile resistance of the concrete. These tensile cracks appeared to be along the flange face at the critical section which is at the midspan. At the same time, cracks developed along the web and started to propagate at an angle of 45^{o} toward the critical section. After the tensile zone had reached the ultimate strain of the concrete, the cracks had almost reached the position of the neutral axis and therefore did not extend any further but increased in width as load was incremented. At the compression side, the cracks expanded and moved rapidly towards the critical section along the web.

No signs of crushing were apparent on the compressive face until ultimate load was achieved. When the ultimate load was reached, failure occured suddenly with the compressive concrete cover falling off. Slight buckling of the compression steel took place in all specimens. In most cases, concrete fell off to a depth of about 1/2 to 1 inch inside the core. All failure were compression failure due to crushing of the concrete and it was believed that buckling of the compression steel was secondary as a result of the crushing of concrete.

It may be noted that one third of all failures took place at the midspan and the remaining were few inches away from the column midheight. Deflections tended to increase more rapidly near the place where failure later occured.

Chapter III

Theoretical model

A. Load-moment-curvature relationships

To determine the strain and curvature distributions across the section the stress-strain relationship for the material has to be defined. In this case it is necessary to determine the stress-strain properties of the constituent materials, i.e., concrete and steel.

The stress-strain curve used in the following analysis accounts for confined and unconfined concrete elements, including the strain softening. The curves shown in figure 3-1 are developed by Cranston and Chatterji's and modified by Hsu.[13]

The experimental stress-strain curve for steel has been idealized using piece wise linear approximation to the curve in the strain hardening region as shown in figure 3-2.

The computation procedure of Hsu's computer program is to assume the load, Ep, Φx and Φy and then iterate until the correct curvatures corresponding to the given P, Mx and My are determined. The convergence is rapid and with a relatively close to initial assumption, convergence can be attained in two or three cycles. The method is ususally also valid for a wild initial guess but the number of necessary iterative cycles becomes larger depending on the accuracy desired.

The convergence method is an extension of the Newton-Raphson method. The details of this computer analysis and

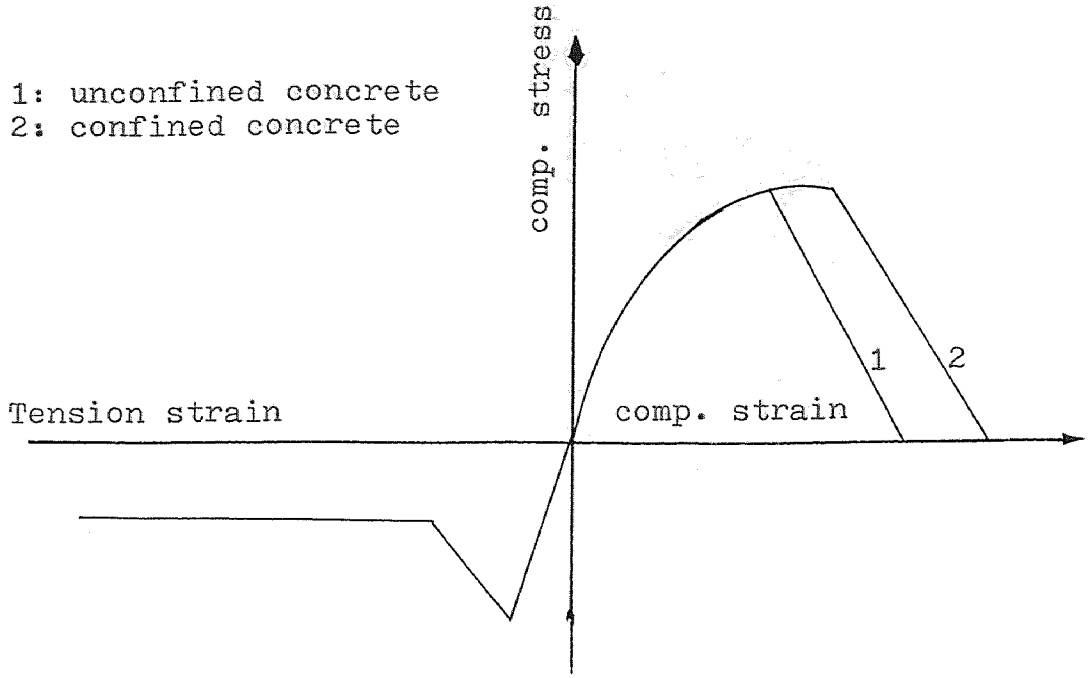

Figure 3-1 Idealized stress-strain curves for concrete

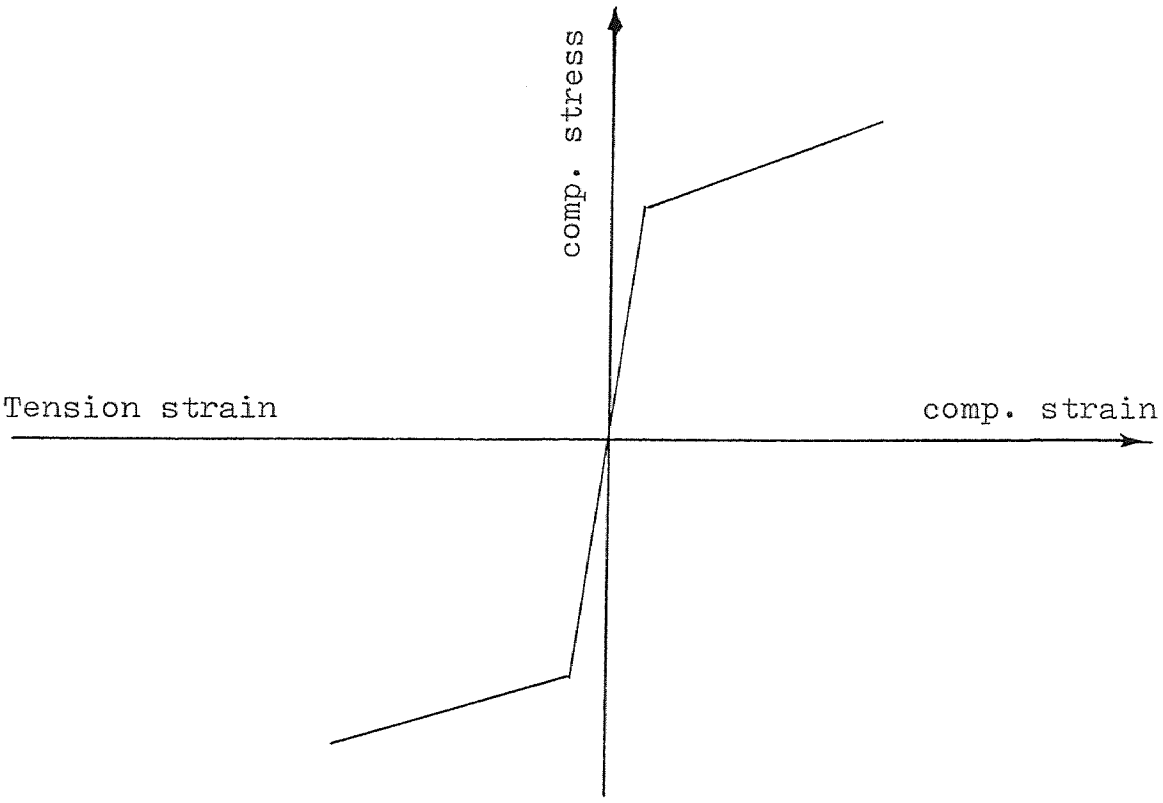

Figure 3-2 Idealized stress-strain curve for steel

program can be found in Ref.(13) by Hsu. A brief description of the method is given below:

The cross section of the structural member is divided into several small elemental areas as shown in figure B-1 and for a given section the stress resultants P, Mx and My can be expressed as functions of curvatures Φx, Φy and strain Ep as follows:

$$\begin{aligned} P &= P(\Phi x, \Phi y, \varepsilon p) \\ Mx &= Mx(\Phi x, \Phi y, \varepsilon p) \\ My &= My(\Phi x, \Phi y, \varepsilon p) \end{aligned} \qquad \text{(I)}$$

By making the assumption that plane sections before bending remain plane after bending, the strain of each element is given by:

$$\varepsilon k = \varepsilon p + \Phi x\ Yk + \Phi y\ Xk$$

Knowing $P_{(c)}$, $Mx_{(c)}$ and $My_{(c)}$ with the corresponding values of Φx, Φy and εp during an iteration cycle, where the subscript (c) denotes calculated values of P, Mx and My obtained in an iteration cycle, equations (1) can be expanded using the Taylor's theorem and neglecting second order and higher terms we get:

$$\begin{aligned} P &= P_{(c)} + \frac{P_{(c)}}{\partial \Phi x}\partial \Phi x + \frac{P_{(c)}}{\partial \Phi y}\partial \Phi y + \frac{P_{(c)}}{\partial \varepsilon p}\partial \varepsilon p \\ Mx &= Mx_{(c)} + \frac{Mx_{(c)}}{\partial \Phi x}\partial \Phi x + \frac{Mx_{(c)}}{\partial \Phi y}\partial \Phi y + \frac{Mx_{(c)}}{\partial \varepsilon p}\partial \varepsilon p \\ My &= My_{(c)} + \frac{My_{(c)}}{\partial \Phi x}\partial \Phi x + \frac{My_{(c)}}{\partial \Phi y}\partial \Phi y + \frac{My_{(c)}}{\partial \varepsilon p}\partial \varepsilon p, \end{aligned} \qquad \text{(2)}$$

where P, Mx and My are the longitudinal load and bending

moment respectively, for which Φx, Φy and $\mathcal{E}p$ are sought. The values $\partial\Phi x$, $\partial\Phi y$ and $\partial\mathcal{E}p$ are increments in Φx, Φy and $\mathcal{E}p$ required to produce P, Mx and My. The partial derivatives are the rates of change of P, Mx and My with Φx, Φy and $\mathcal{E}p$. Now the partial derivatives in Equation (2) are replaced by the corresponding difference quotients, and by incrementing one deformation quantity at a time, the rates of change can be evaluated, then the simultaneous equation (2) are solved and $\partial\Phi x$, $\partial\Phi y$ and $\partial\mathcal{E}p$ are determined. These increments are added to the initial deformations and the process is repeated using the new deformation values until convergence is obtained.

B. Load-deflection relationships

Hsu[13] modified the moment-area theorems and derived the following equations to evaluate the control deflection components $2x$ and $2y$ of the biaxially loaded pin-ended short columns.

$$\delta_{2x} = \Phi_y l^2/8$$
$$\delta_{2y} = \Phi_x l^2/8$$

The computer program did not account for the column deflection, the axial load is reduced to its actual value by using the following equation:

$$P_3 = \frac{P(ex^2 + ey^2)^{1/2}}{((ex + \delta_{2y})^2 + (ey + \delta_{2x})^2)^{1/2}}$$

Chapter IV

Tee Column Test Results

After completion of the testing, all data were reduced, analysed and evaluated.

The experimental and analytical values of the moments, curvatures, axial loads and deflections at failure are presented in table 4-1 for each tee column test.

A typical relationship between moment-curvature and load-deflection curves for short columns are presented in figure 4-1.

The analytical results are determined by means of a computer program which is outlined briefly in this report and available in Ref.(13).

All element areas and coordinates, average concrete ultimate compressive strength, steel stress-strain curve, cross section dimensions and eccentricities were used as input data for the computer program. The output features were the moment-curvatures Mx- Φx, My- Φy and the axial load P.

For the experimental results, the measurements of all instruments could not be taken at failure so the final moments, curvatures and deflections required extrapolation.

The moment was computed as produced by the deflection of the column under load plus the eccentricity of the axial load with respect to the cross section centroid. The curvature was computed at the various stages of load application from the measured average concrete compressive strains versus the distance between the Demec gauges located either on the flange or the web plane across the critical cross section of the

Table 4-1 Specimens at failure forces

Specimen	Eccentricity ex	Eccentricity ey	Experimental: Deflection δ_x	Experimental: Deflection δ_y	Experimental: Moment Mx	Experimental: Moment My	Experimental: Curvature Φ_x	Experimental: Curvature Φ_y	Experimental: Axial load P_3	Theoretical: Deflection δ_{2x}	Theoretical: Deflection δ_{2y}	Theoretical: Moment Mx	Theoretical: Moment My	Theoretical: Curvature Φ_x	Theoretical: Curvature Φ_y	Theoretical: Axial load P_3
	in		in		in-k		1/in		k	in		in-k		1/in		k
T-1	2.37	2.50	0.383	0.525	321.9	296.9	1050	665	108.30	0.366	0.622	267.3	253.9	960	566	106.92
T-2	7.43	1.50	0.720	0.248	84.8	395.4	390	1410	48.48	0.792	0.224	66.2	328.0	350	1230	44.00
T-3	2.09	2.18	0.400	0.484	375.6	337.8	1260	735	139.25	0.321	0.550	260.3	249.0	893	513	118.92
T-4	2.31	2.37	0.386	0.450	329.2	314.6	800	608	123.78	0.366	0.550	304.0	296.0	853	565	127.93
T-5	5.80	1.12	0.730	0.180	89.1	442.3	440	1700	69.10	0.674	0.191	69.7	359.7	350	1400	62.00
T-6	3.00	0.56	0.603	0.106	87.7	455.0	150	1173	128.94	0.646	0.080	71.7	384.3	120	998	128.07

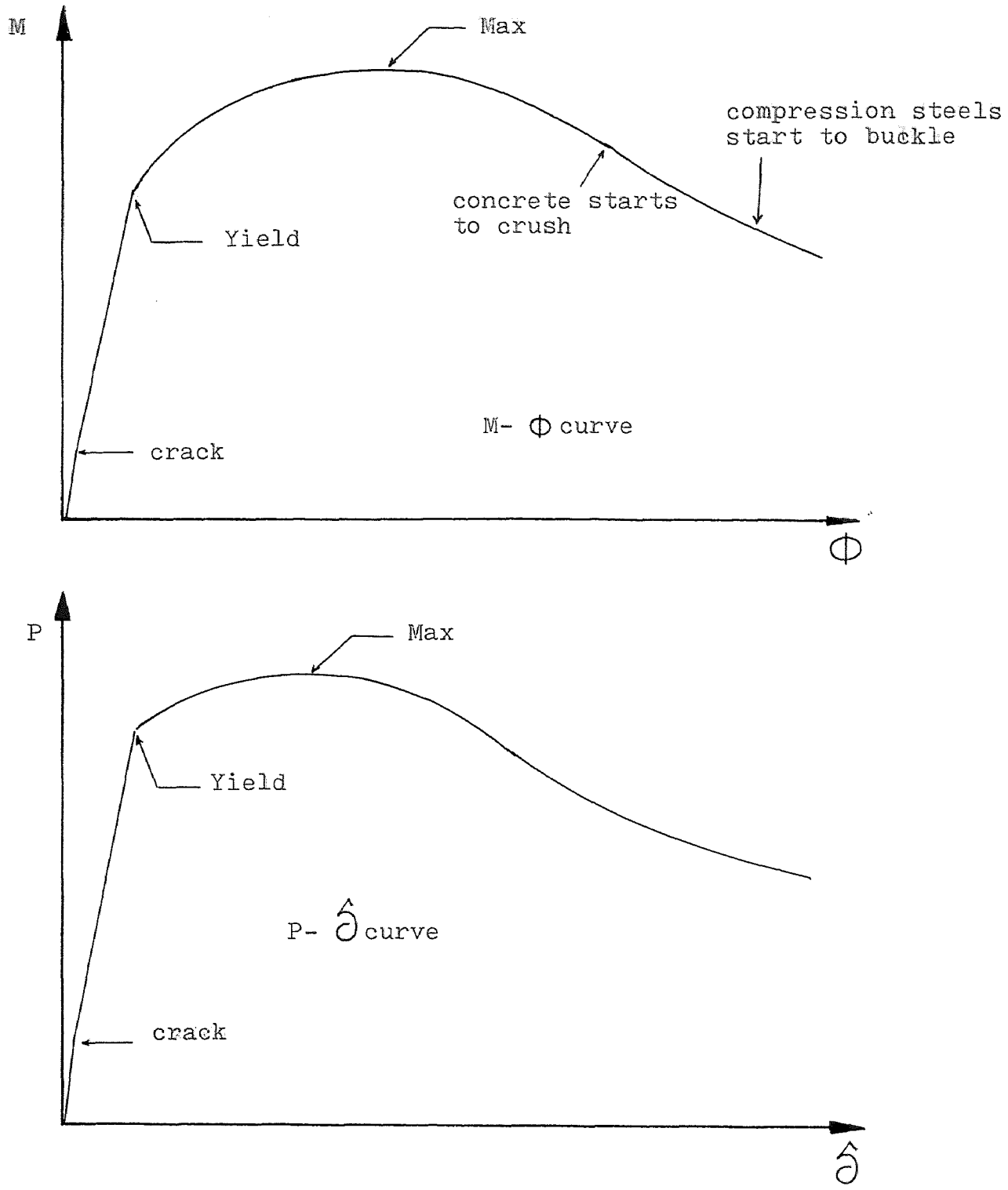

Figure 4-1 Typical relationship between moment-curvature and load-deflection curves for short columns

column. A least squares linear curve fit was made to the averages of these measured concrete compressive strains and the curvature was computed at each loading stage by dividing the maximum concrete compressive strain to its distance where the linear curve bisected the zero-strain axis. The web and flange curvatures of each principal axis at any particular load were averaged and used to plot the moment-curvature curves. The curvature between the web and flange, at a constant load, differs at most by a margin of 5%.

For clarity, a complete set of calculations for specimen T-5, shows the interpretation of the data. At each load stage, strain distribution across the section, the moment curvature and load deflection curves are plotted. The computations and curves for specimen T-5 are showed at the end of chapter IV. Tables and figures for the remaining specimens are presented in appendix A.

The theoretical and experimental curves have been plotted with dashed and solid lines respectively in all figures for comparison over the full range of the column behavior. Also, comparison between the experimental and analytical ultimate loads, moments, curvatures and deflections in the form of ratios were made for the six tested tee columns.

The results show mean values for $M_{xe}/M_{xt} = 1.24$, with a range from 1.08 to 1.44, for $\Phi_{xe}/\Phi_{xt} = 1.17$, with a range from 0.94 to 1.41. The ratios for M_{ye}/M_{yt} and Φ_{ye}/Φ_{yt} showed a similar deviation with the mean values equal 1.20, with a range from 1.06 to 1.35 and 1.20, with a range from 1.07 to

Table 4-2 Comparison of theoretical and test results

Specimens	$\frac{MxE}{MxT}$	$\frac{\Phi xE}{\Phi xT}$	$\frac{MyE}{MyT}$	$\frac{\Phi yE}{\Phi yT}$	$\frac{\delta x}{\delta 2x}$	$\frac{\delta y}{\delta 2y}$	$\frac{PE}{PT}$
T-1	1.20	1.10	1.16	1.17	1.04	0.85	1.01
T-2	1.28	1.11	1.20	1.14	0.91	1.11	1.10
T-3	1.44	1.41	1.35	1.43	1.24	0.88	1.17
T-4	1.08	0.94	1.06	1.07	1.06	0.82	0.93
T-5	1.27	1.25	1.22	1.21	1.08	0.95	1.11
T-6	1.22	1.25	1.18	1.17	0.93	1.32	1.01
Summary	1.24	1.17	1.20	1.20	1.04	0.98	1.05

E - experimental

T - theoretical

1.43 respectively. The mean value for Pe/Pt = 1.05, with a range from 0.96 to 1.17. The ratios for $\delta x/\delta 2x$ and $\delta y/\delta 2y$ are close to unity, similar to the axial load ratio, with the mean values equal to 1.04 and 0.98 respectively.

Table 4-3 Strain distribution test results at various loads for specimen T-5

Loads (psi)	Demec guages #												
	1	2	3	4	5	6	7	8	9	10	11	12	13
10.31	366	366	266	450	283	233	250	183	50	16	-50	-333	-383
20.63	700	950	766	966	766	466	483	466	416	150	33	-833	-800
30.94	1150	1450	1300	1366	1066	633	816	700	666	250	33	-1000	-1416
41.26	1700	2050	1983	1816	1333	1000	1083	1033	833	366	116	-2216	-1916
46.41	1950	2283	2250	2033	1400	1175	1333	1283	1000	416	116	-1916	-2250
51.57	2283	2616	2500	2083	1566	1516	1416	1450	1166	583	116	-1833	-2500
56.73	2700	2983	2950	2616	1983	1633	1733	1783	1416	666	216	-2216	-2900
61.89	3400	3750	3916	3566	2566	2133	2083	2200	1833	833	116	-2950	-4000
67.10	3850	4416	4500	4116	2800	2216	2416	2450	1950	883	-50	-3583	-4666
69.10	Failure												

Strains are multiplied by a factor of ($\times 10^{-6}$)
(-) denotes tension

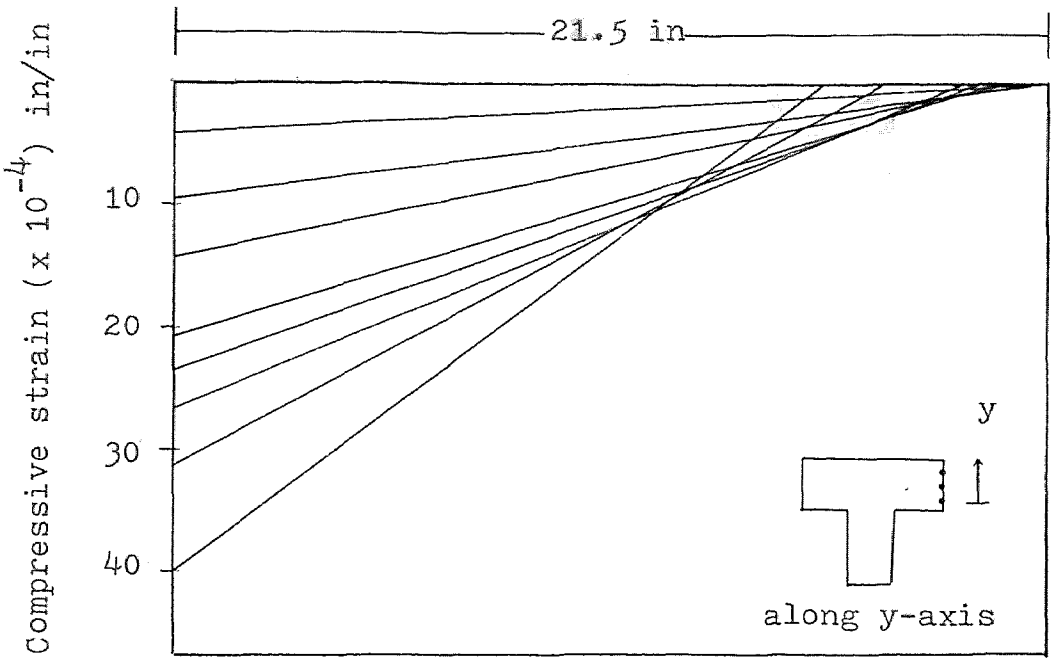

Strain distribution across the flange

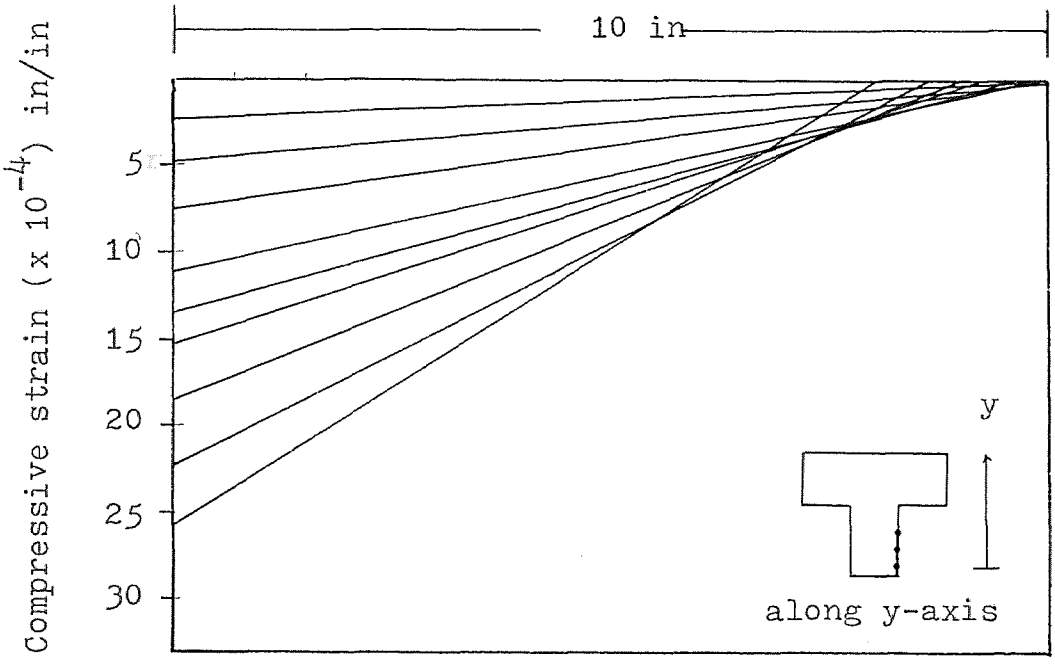

Strain distribution across the web

Figure 4-2a Strain distribution across the section for specimen T-5

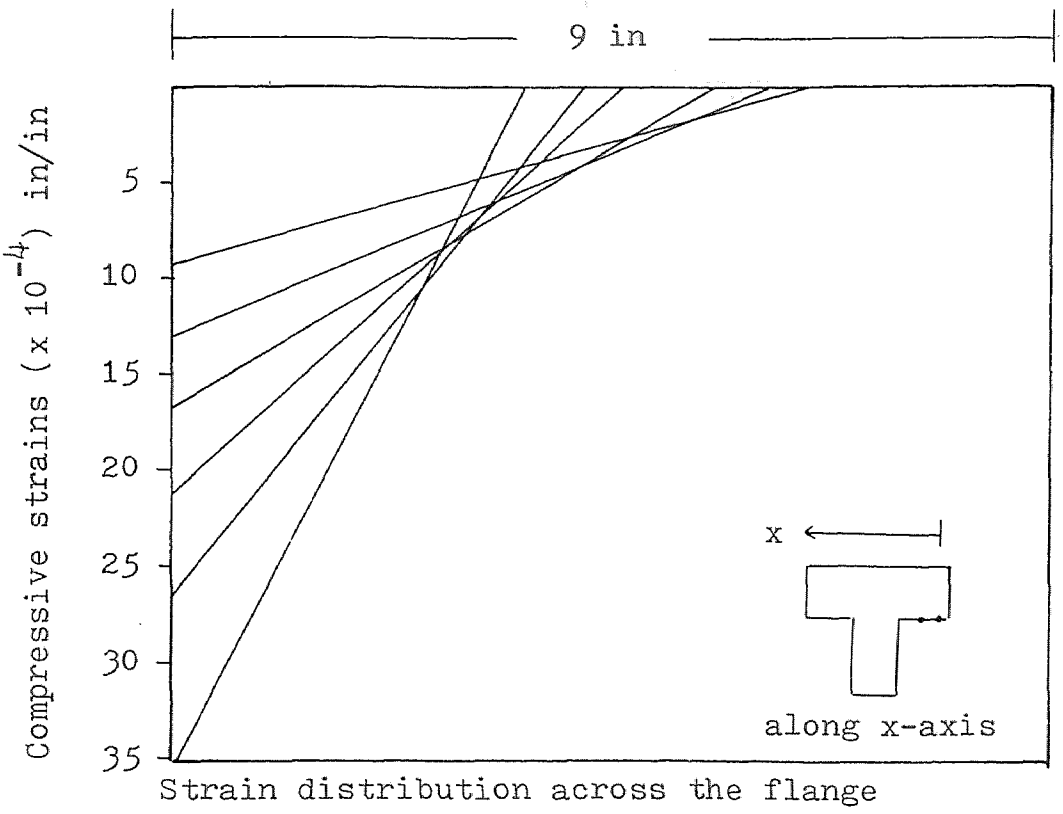

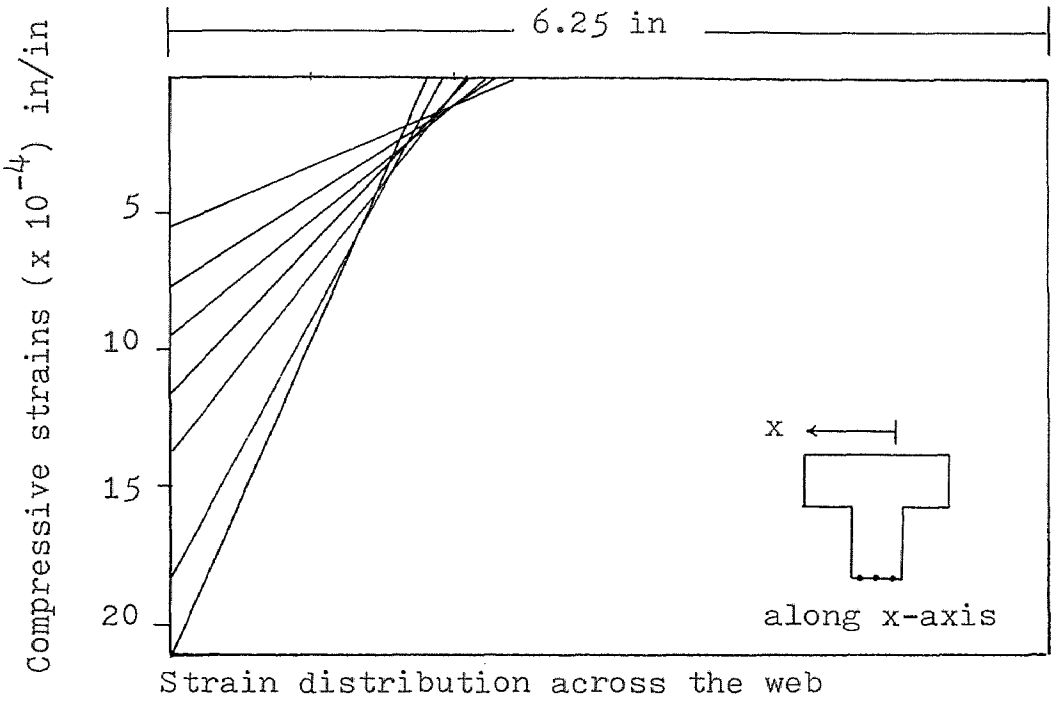

Figure 4-2b Strain distribution across the section for specimen T-5

Table 4-4 Load-deflection results along x-axis for specimen T-5

Loads	Experimental			Theoretical
	$\delta_x(1)$*	$\delta_x(2)$*	$\delta_{x\,AVG}$	δ_{2x}
kips	in	in	in	in
20.63	0.068	---	0.068	0.070
30.94	0.147	0.080	0.113	0.120
41.26	0.228	0.138	0.183	0.190
46.41	0.271	0.174	0.223	0.235
51.57	0.318	0.197	0.258	0.320
56.73	0.382	0.254	0.318	0.880 F
61.89	0.528	0.413	0.471	
67.10	0.628	0.503	0.566	
68.07	Failure			

(1)* denotes reading from Ames dial #1
(2)* denotes reading from Ames dial #2
F failure

Table 4-5 Load-deflection results along y-axis for specimen T-5

Loads	Experimental			Theoretical
	$\delta_{x(1)}$*	$\delta_{x(2)}$*	$\delta_{x\ avg}$	δ_{2x}
kips	in	in	in	in
20.63	0.032	0.033	0.033	0.030
30.94	0.054	0.037	0.045	0.042
41.26	0.073	0.052	0.063	0.060
46.41	0.080	0.055	0.068	0.077
51.57	0.084	0.083	0.084	0.100
56.73	0.099	0.084	0.092	0.210 F
61.89	0.130	0.135	0.133	
67.10	0.156	---	0.156	
68.07	Failure			

(1)* denotes reading from Ames dial #1
(2)* denotes reading from Ames dial #2
F denotes failure

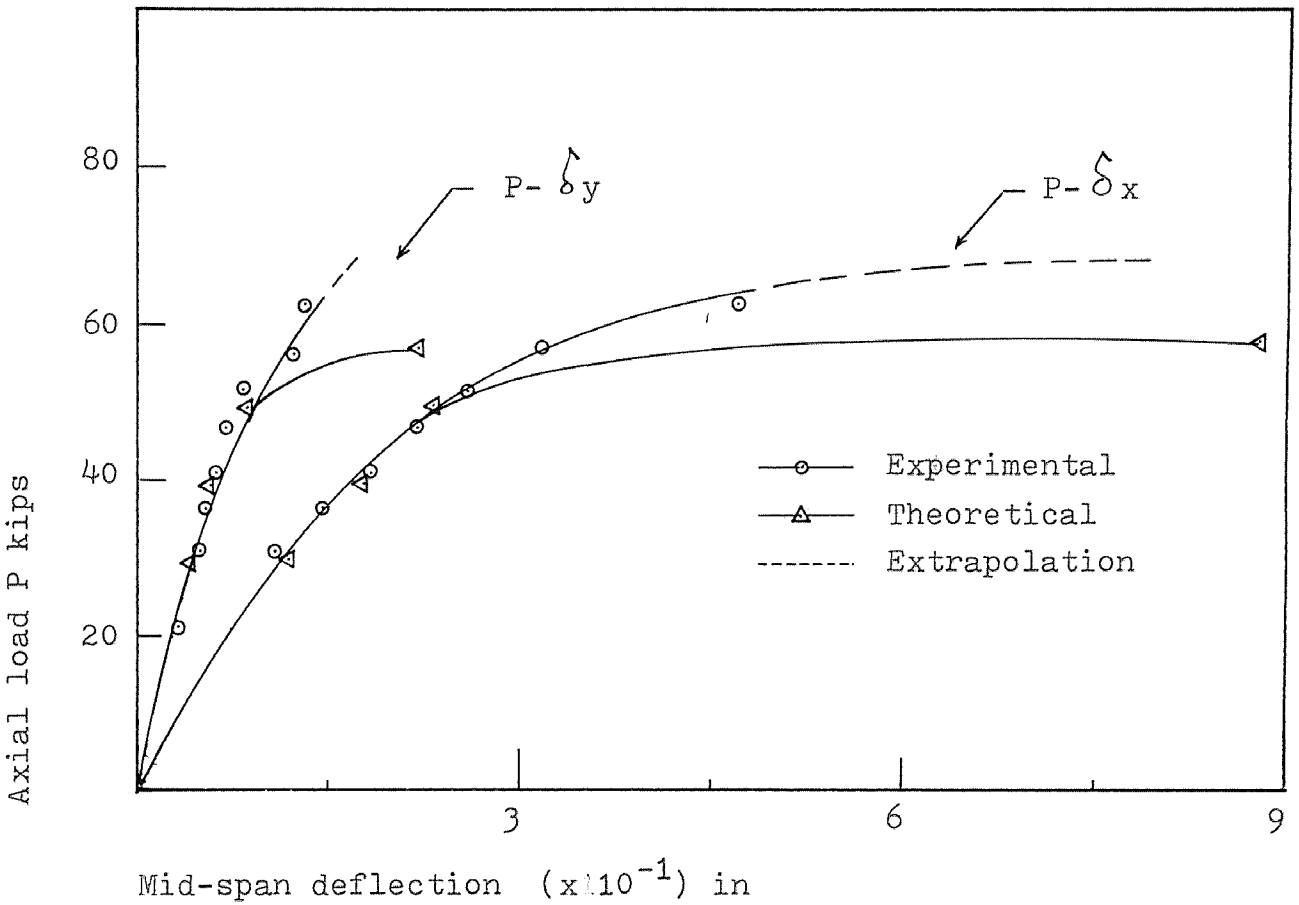

Figure 4-3 Load-deflection curves for specimen T-5

Table 4-6 Biaxial moment-curvature results for specimen T-5

Experimental					Theoretical				
Loads	Mx	Φx	My	Φy	Loads	Mx	Φx	My	Φy
kips	in-k	1/in	in-k	1/in	kips	in-k	1/in	in-k	1/in
10.31	11.75	20	---	---	20.00	22.50	43	116.00	132
20.63	23.72	43	120.94	140	25.00	28.12	54	145.01	168
30.94	36.19	72	183.01	218	30.00	33.75	66	174.00	205
41.26	48.89	105	242.50	304	40.00	45.00	91	232.02	285
46.41	55.69	129	279.62	398	50.00	56.25	131	290.04	419
51.57	62.65	150	313.41	483	55.00	61.88	174	319.04	589
56.73	69.91	193	348.32	640	60.00	67.29	345	347.98	1362
61.89	77.67	256	384.95	970					
67.04	86.48	320	430.70	1240					
68.07	88.49	---	445.85	---					

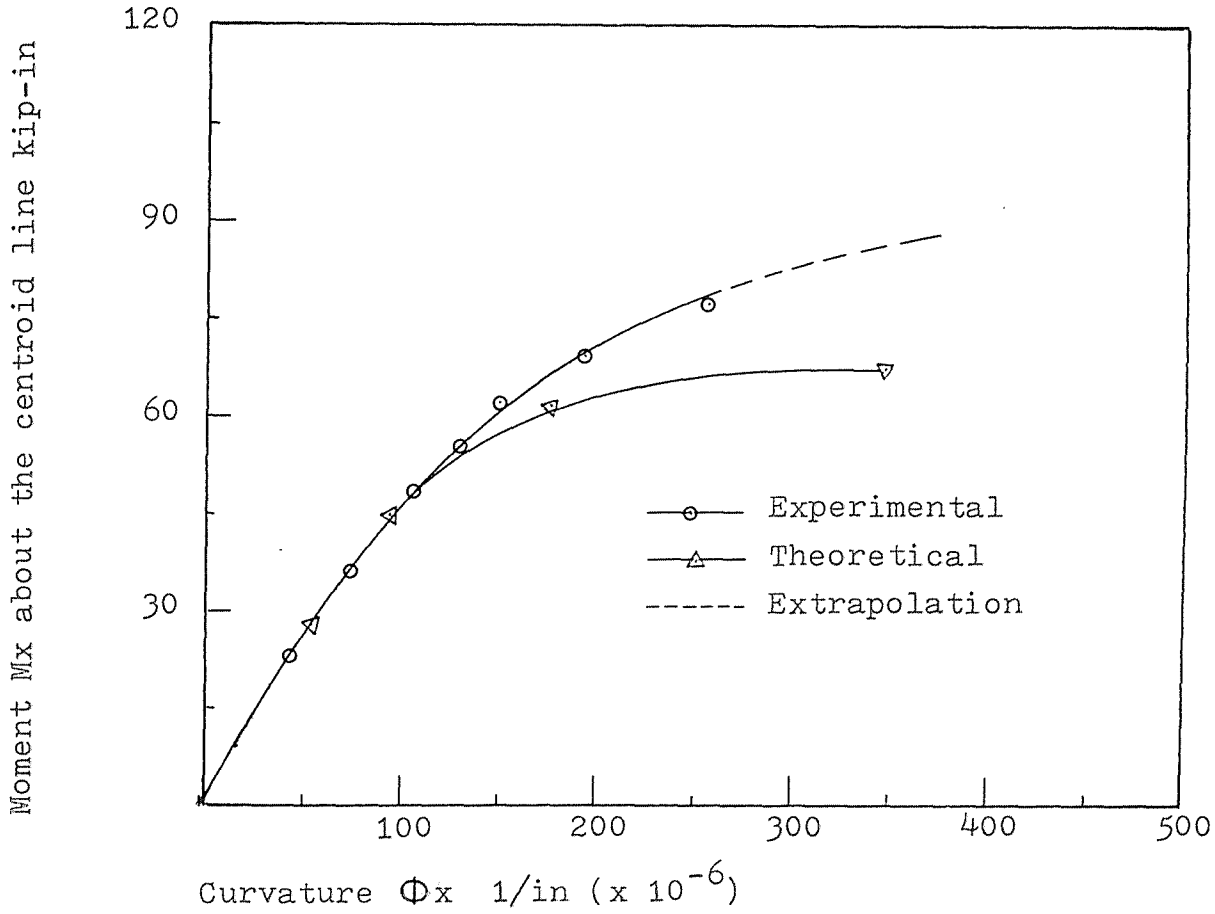

Figure 4-4a Biaxial moment-curvature curves for specimen T-5

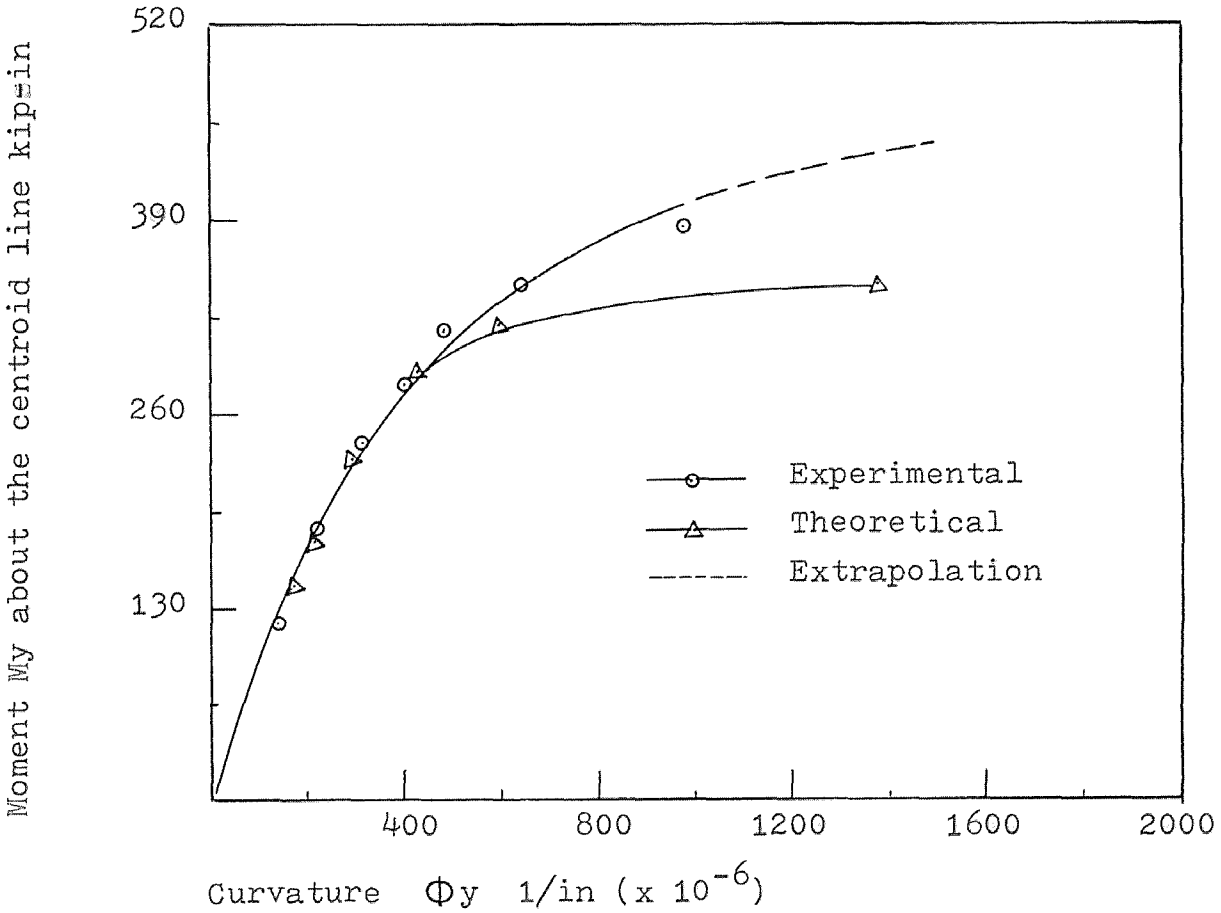

Figure 4-4b Biaxial moment-curvature curves for specimen T-5

Chapter V

Discussion and Conclusions

The elastic and inelastic behavior of tee column members can be described by means of moment-curvature and load-deflection relationships. The analytical approach used tends to underestimate slightly the axial load, moments and curvatures at failure. The average values of all specimens for Mxe/Mxt, Φxe/Φxt, Mye/Myt and Φye/Φyt are 1.24, 1.17, 1.20 and 1.20 respectively. The axial load and deflections showed smaller deviations with Pe/Pt, δx/δ2x and δy/δ2y equal to 1.07, 1.04 and 0.98 respectively. It should be noted that the analytical results of specimen T-3 underestimated the moment curvature and axial load experimental results by 30 and 20 percent respectively. The reason is that the specimen T-3 was tested up to 75 percent of its capacity, then reloaded and retested again the following day until failure. The error margin of the overall mean values could be reduced if specimen T-3 is neglected.

Based on present studies, a satisfactory agreement between the analytical and experimental results is achieved. Some of the variations between the analysis and test results are due to the experimental errors in locating the eccentricities which are likely to affect the magnitude of the tested loads. The eccentricities could have varied within $\pm$ 0.5 inch. Similarly, the dimensions of the cross sections could have varied by the same margin as the columns were cast in plywood molds.

On the average, the secondary moments about both principal axes account for five percent at 70 percent of the column capa-

city, and is increased to ten percent at failure load. The secondary moments, induced by deflections, cause the pin-ended short tee column to fail at the midspan, where the moments are maximum, but four out of six tested specimens failed few inches away from the center of the specimen. This argument shows that material effect is more significant than the deflection effect in short tee columns. In general, the secondary moments have little effect on short columns which can be neglected for practical purposes.

It is observed from the moment curvature and load deflection curves for specimens T-2 and T-5 under large eccentricities, that fairly good agreement exists between the theoretical and actual curves up to 70 percent of the column capacity but the analytical curves deviate to the conservative side when approaching to failure. The analytical resuts underestimate the column capacity by 20 percent which, of course, is no cause for concern.

From the present studies, one can conclude that the computer analysis and results are on the conservative side in predicting the ultimate load, the moments and curvatures for biaxially loaded columns with small and large eccentricities, respectively.

From the moment-curvature figures, it can be seen that as the axial load is increased, the slope of the moment-cuvature relationship decreases slightly up to the stage

where the column carries almost 65 percent of its capacity. This indicates that the column stiffness is reduced over this range of loading. At that level, the analytical and experimental curves behaved similarly with a margin of 5 percent error. For higher loads, the slope decreases rapidly, reaching the stage where the curvature increases without any further increase of the bending moment, thus leading to failure. At the final stages, the analytical approach developed by Hsu can predict the above behavior but slightly underestimated the ultimate moments and curvatures for all columns.

The experimental and analytical load-deflection curves behave similarly through all the load stages with a margin of 5 percent error. In both cases, the rate of increase for the column deflection with axial load increases more than that at the lower loads, leading to the stage where the column suffers enormous deformation at a constant load and eventually arrives at the point of destruction.

The inelastic behavior, which can be deduced form the ductility and deformation results of moment-curvature curves, has formed the basis of the redistribution of the moments and forces in a statistically indeterminate structure, and these characteristics can also be found useful for the limit analysis and design of reinforced concrete structures.

Good agreement was obtained between the experimental loads, strengths and analytical resutls calculated using the computer

program developed by Hsu. The experimental curvatures and deflections were in good agreement with the analytical results through all load stages from zero load up to the maximum moment capacity of the section.

Design aids for tee-shaped reinforced concrete columns could become available once the exponent of the ratios between moment components and moment capacities about each principal axis is determined form the results of this investigation.

Finally, the mathematical model developed by Hsu has been experimentally verified as suitable for analysis of tee-shaped reinforced concrete columns under combined biaxial bending and axial compression. Based on this mathematical model, one can study the strength behavior, load-moment interaction diagrams and three dimensional failure surface for tee-shaped reinforced concrete columns.

Appendix A

Tables and Figures for all Specimens

Table A-1 Strain distribution test results at various loads for specimen T-1

Loads	Demec gauges #									
	1	2	3	4	7	8	11	12	13	14
20.63	-133	-316	-216	-233	200	316	316	216	366	283
30.94	-250	-433	-300	----	383	616	365	500	550	433
41.26	-383	-583	-450	-366	666	750	533	683	766	600
51.57	-750	-850	-566	-466	816	1100	883	766	950	816
61.89	----	-1066	-716	-533	1033	1400	1133	1116	1316	933
72.20	-966	-1233	-916	-700	1266	1650	1250	1650	1516	966
82.52	-1700	-2400	----	-783	1516	2050	1550	1916	1833	1183
92.83	-2466	-3350	-1300	-966	2416	2766	1866	2333	2416	1516
103.15	-2850	-3693	-1433	-1150	3366	----	2400	3066	----	----
108.30	Failure									

All units are x 10^{-6}
(-) denotes tension

Table A-2 Strain distribution test results at various loads for specimen T-2

Loads kips	Demec gauges #							
	3	4	7	8	5	6	11	10
4.12	816	750	533	566	850	566	-1016	233
20.63	1400	983	933	816	1400	1166	-1466	---
25.78	1650	1816	1000	866	1650	1283	-1966	183
30.94	1966	2100	1200	1000	1883	1333	-2583	433
36.10	2183	2483	1350	1200	2316	1700	-2916	450
41.26	3000	3483	1850	1983	2933	2183	-3683	483
46.41	4016	4466	2450	2150	4100	3083	-4383	566
48.48	Failure							

Strains are multiplied by a factor of ($\times 10^{-6}$)

(-) denotes tension

Table A-3 Strain distribution test results at various loads for specimen T-3

Loads (kips)	Demec gauges #										
	1	2	3	4	5	6	7	8	10	11	12
20.63	400	483	450	500	316	433	666	550	-100	-300	--
30.94	650	566	683	633	616	550	983	633	-133	-383	-83
41.26	766	850	950	950	733	933	1250	816	-266	-583	-216
51.57	933	1033	1166	1150	966	1000	1533	1100	-466	-633	-416
61.89	983	1183	1300	1316	1050	1400	1716	1250	-550	-700	-583
72.20	1116	1433	1516	1566	1216	1600	1966	1466	-683	-766	-683
82.52	1283	1600	1733	1716	1400	2016	2216	1633	-700	-850	-833
92.83	1483	1800	1900	1916	1566	2183	2450	1800	-600	-916	-1016
103.15	1600	2066	2166	2000	1850	2383	2766	2100	----	-1300	-1216
113.46	1733	2150	2566	2366	1983	2850	3266	2483	-550	-1050	-1766
123.78	1850	2483	2666	2616	2300	3266	3700	2916	-466	-1683	-1950
134.09	2100	3233	3333	3500	2900	4100	5016	4033	-583	-1550	-3283
139.25	Failure										

Strains are multiplied by a factor of (x 10^{-6})
(-) denotes tension

Table A-4 Strain distribution test results at various loads for specimen T-4

Loads (kips)	Demec gauges #										
	1	2	3	4	5	6	7	8	10	11	12
20.63	200	183	550	450	283	500	400	333	116	---	233
30.94	233	516	766	650	666	716	516	466	166	116	66
41.26	400	683	966	866	700	866	766	633	50	16	-166
51.57	466	716	1050	1166	883	1166	1033	750	-166	----	-333
61.89	600	816	1250	1400	1000	1300	1216	966	-283	-383	-583
72.20	700	933	1383	1250	1250	1583	1416	1050	-416	-550	-1050
82.52	816	1200	1750	1450	1500	1833	1683	1300	-500	-633	-1333
92.83	900	1366	1783	1566	1650	2166	1933	1383	-666	-966	-1533
103.15	1150	1666	2133	1683	1833	2500	2350	1700	-800	-1133	-2383
113.46	1316	1883	2383	1733	1933	2833	2666	1750	-916	-1166	-2416
118.62	Failure										

Strains are multiplied by a factor of ($\times 10^{-6}$)
(-) denotes tension

Table A-5 Strain distribution test results at various loads for specimen T-6

Loads (kips)	Demec gauges #										
	1	2	3	6	7	8	9	10	11	12	13
10.31	200	283	283	266	283	250	183	66	66	-166	266
30.94	733	750	750	816	883	766	333	283	100	-433	-800
51.57	1200	1283	1366	1366	1483	1500	483	450	150	-666	-1300
72.20	1700	1833	1950	1916	2066	2100	766	666	200	-833	-1916
92.83	2366	2366	2283	2483	2666	2733	1350	1050	450	-1200	-2250
103.15	2583	2666	2583	2733	2950	3050	1733	1116	483	-1333	-2300
113.46	3116	3283	3366	3066	3250	3580	2050	1466	616	-1583	-2933
123.78	3566	3750	3783	3283	3566	----	2216	1650	700	-1916	-3216
128.93	Failure										

Strains are multiplied by a factor of (x 10^{-6})
(-) denotes tension

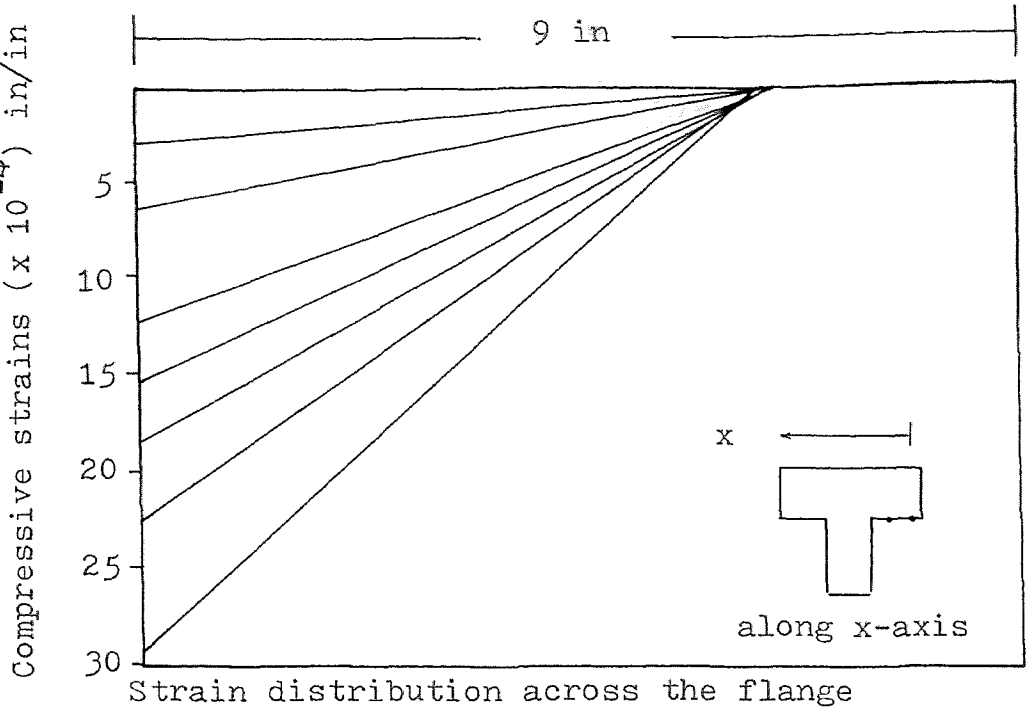

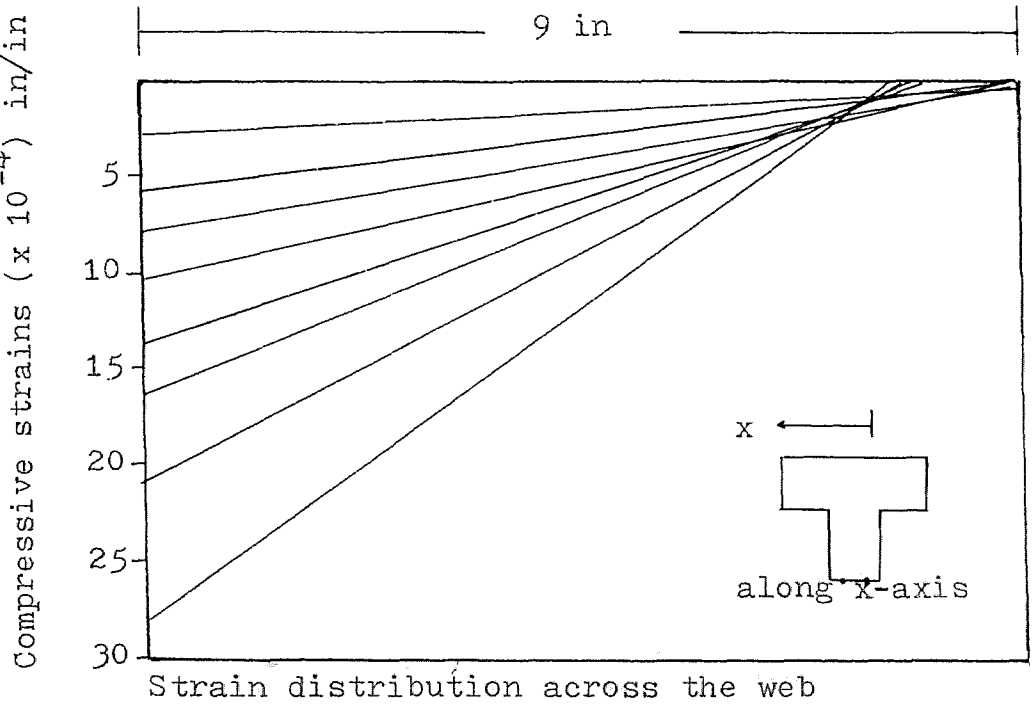

Figure A-1b Strain distribution across the section for specimen T-6

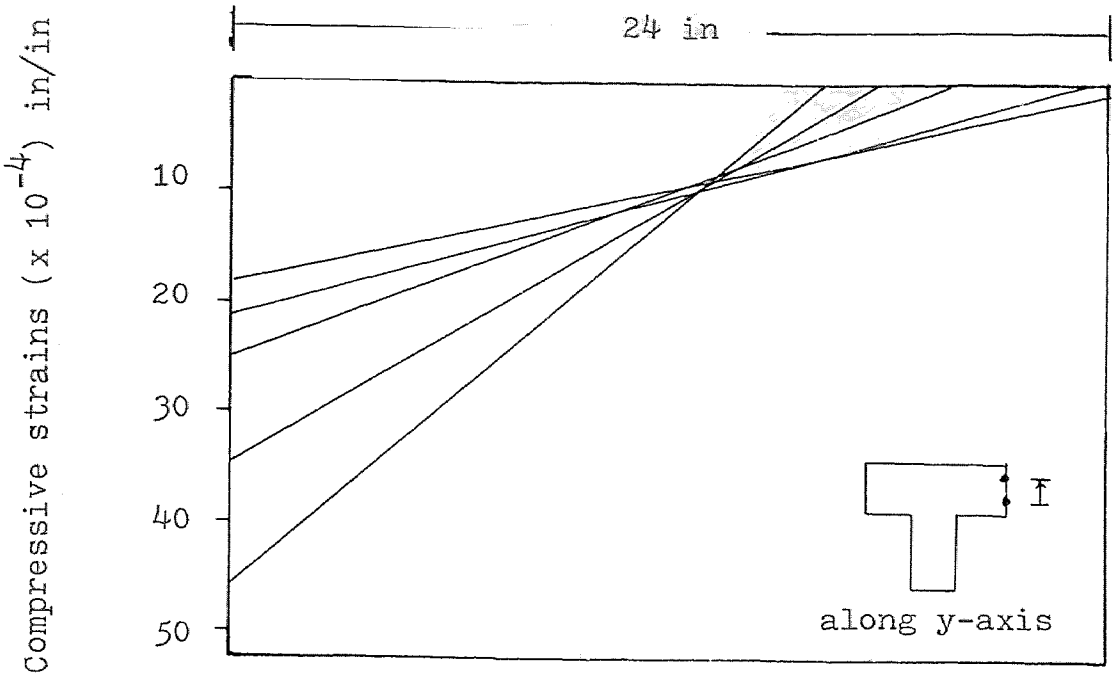

Strain distribution across the flange

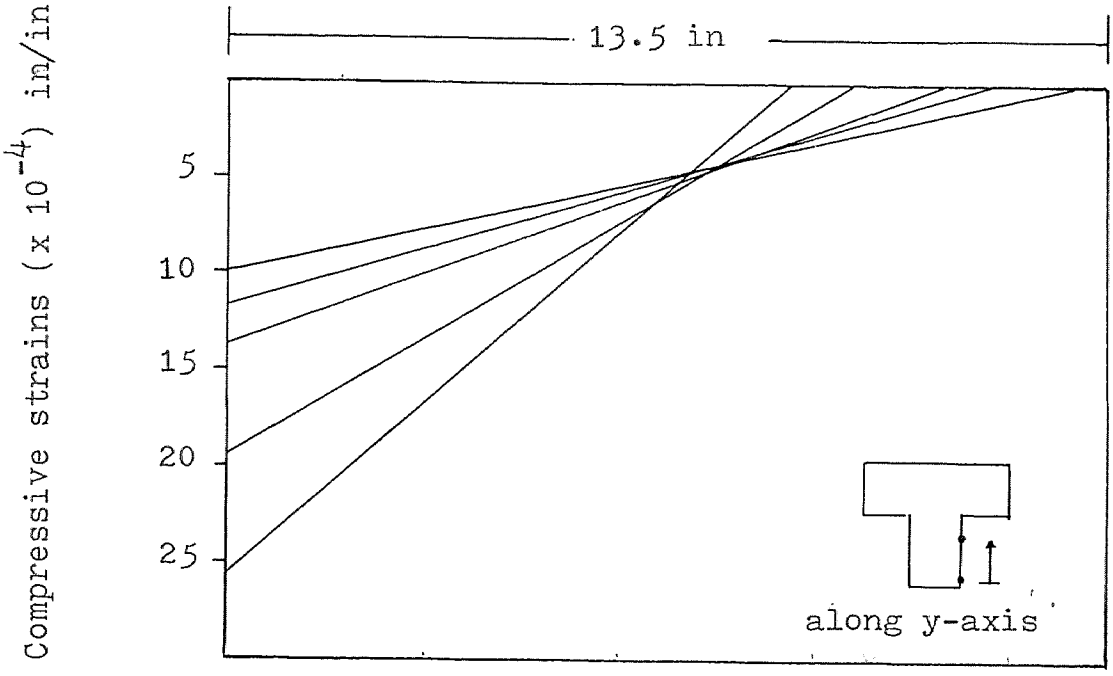

Strain distribution across the web

Figure A-2a Strain distribution across the section for specimen T-2

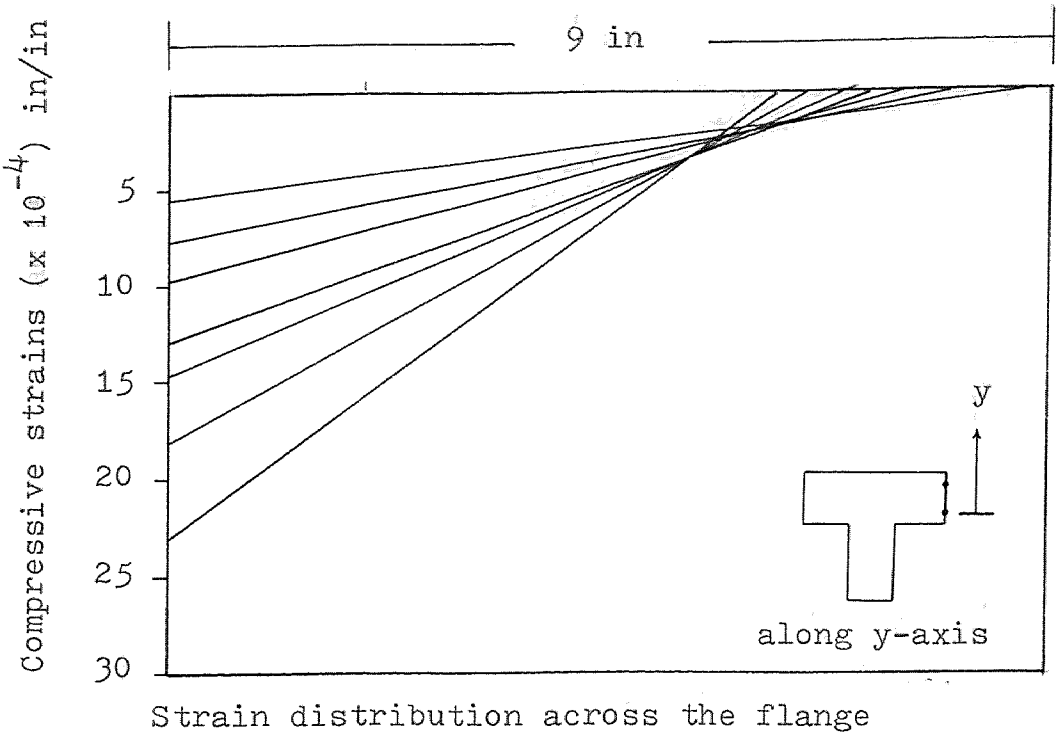

Figure A-1a Strain distribution across the section for specimen T-1

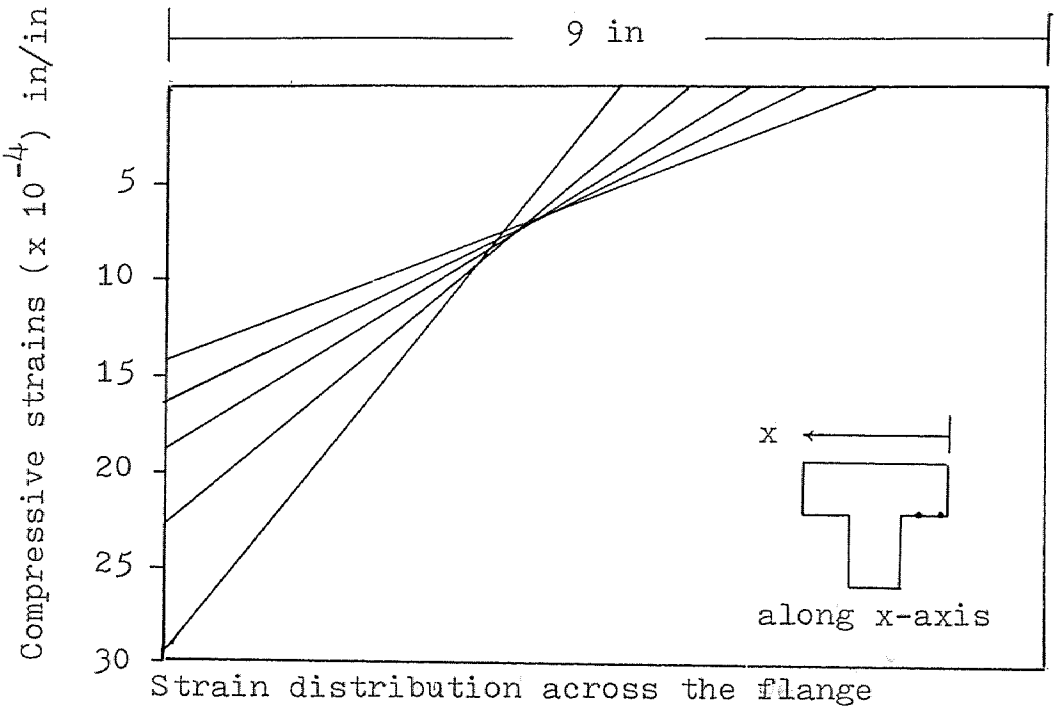

Figure A-2b Strain distribution across the section for specimen T-2

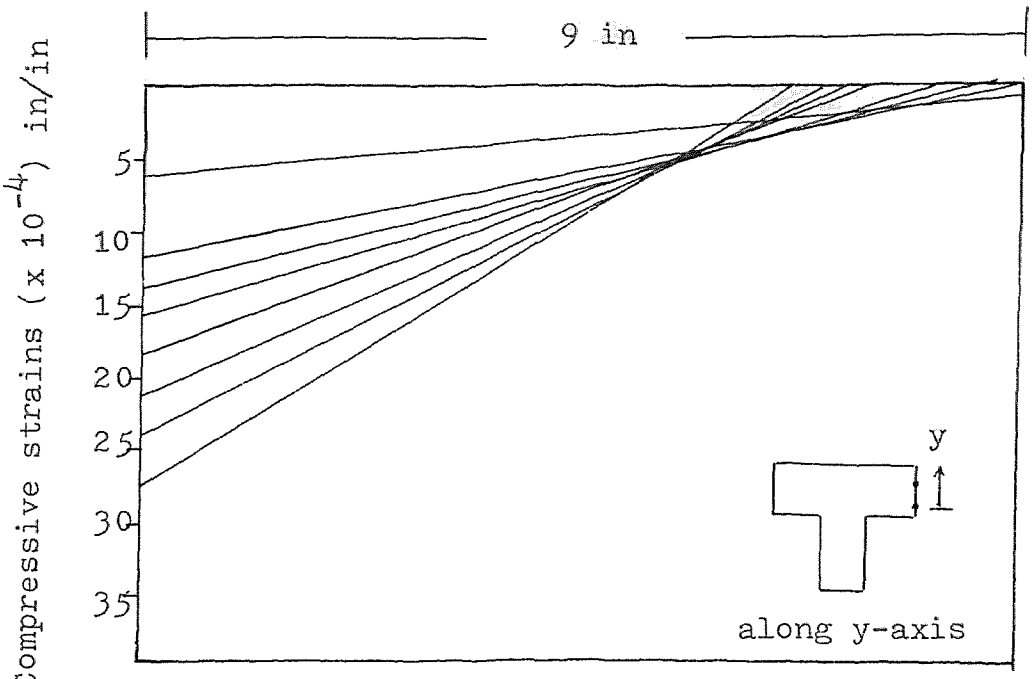

Strain distribution across the flange

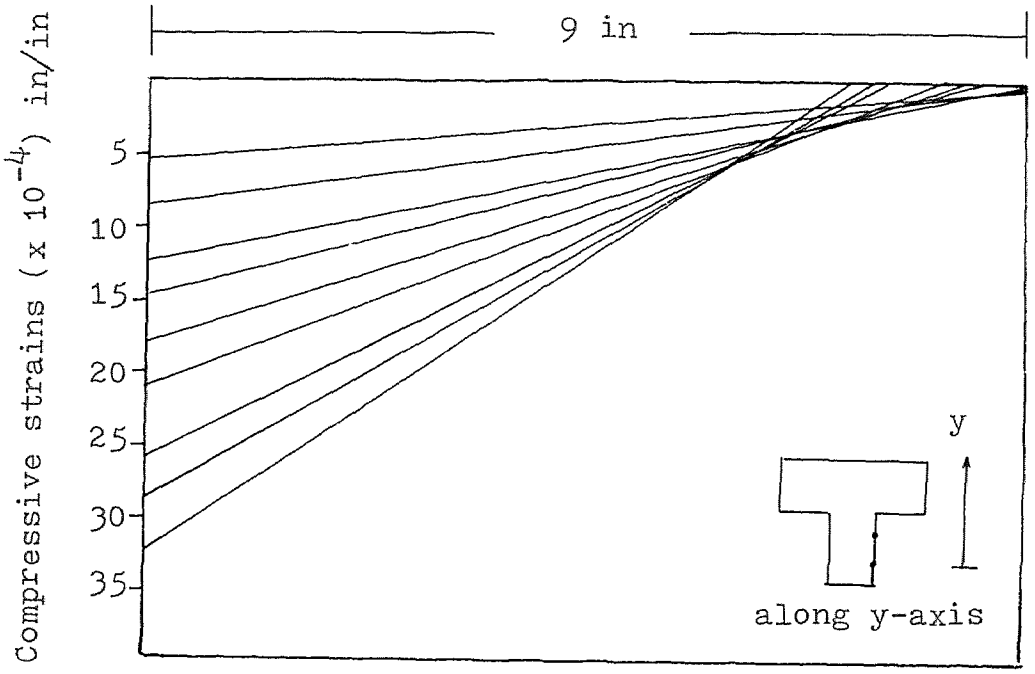

Strain distribution across the web

Figure A-3a Strain distribution across the section for specimen T-3

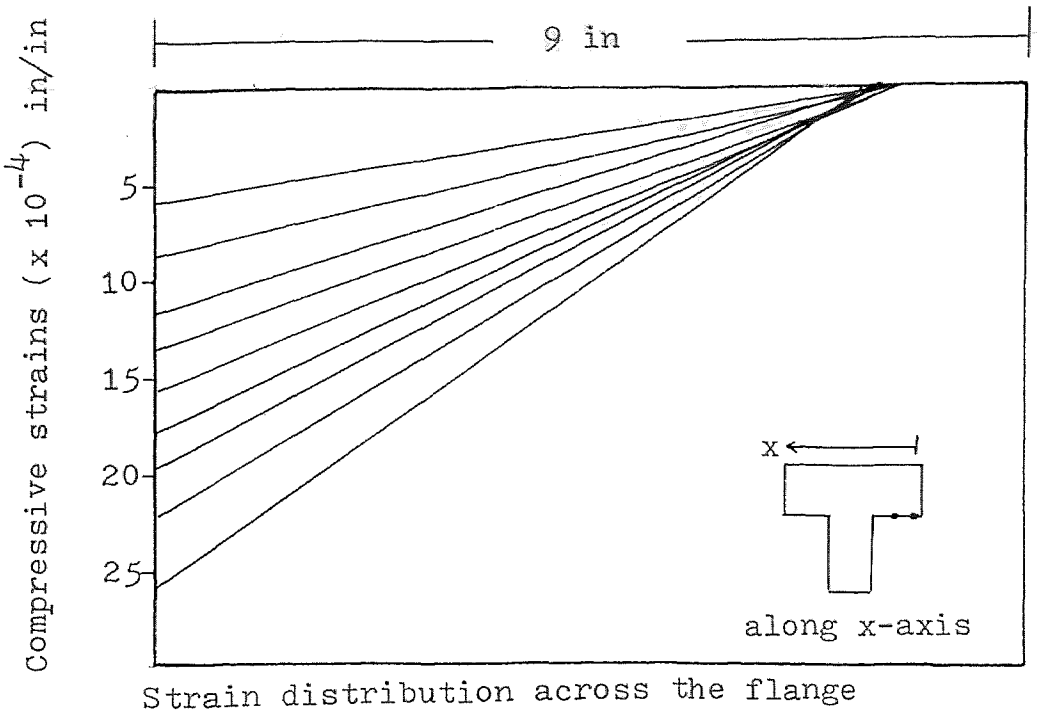

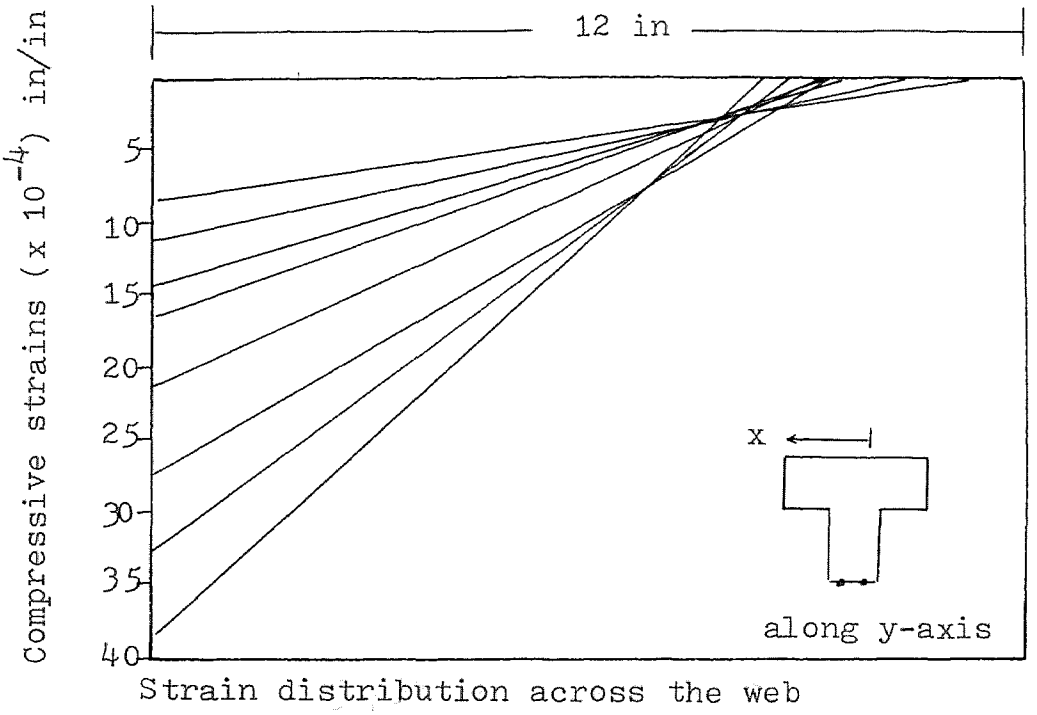

Figure A-3b Strain distribution across the section for specimen T-3

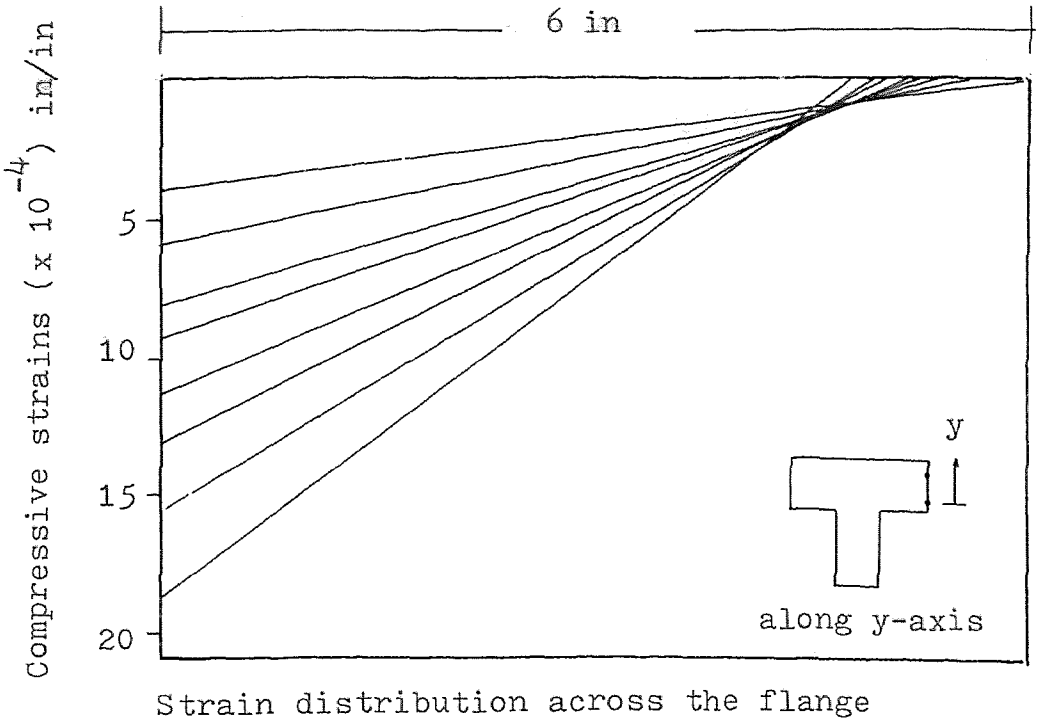

Strain distribution across the flange

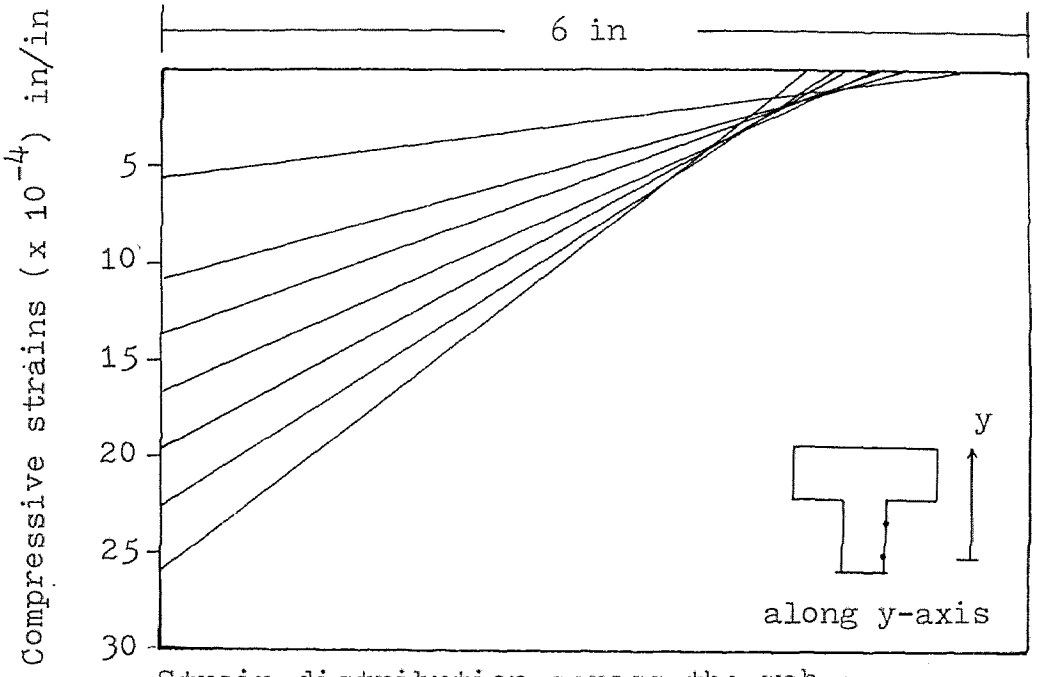

Strain distribution across the web

Figure A-4a Strain distribution across the section for specimen T-6

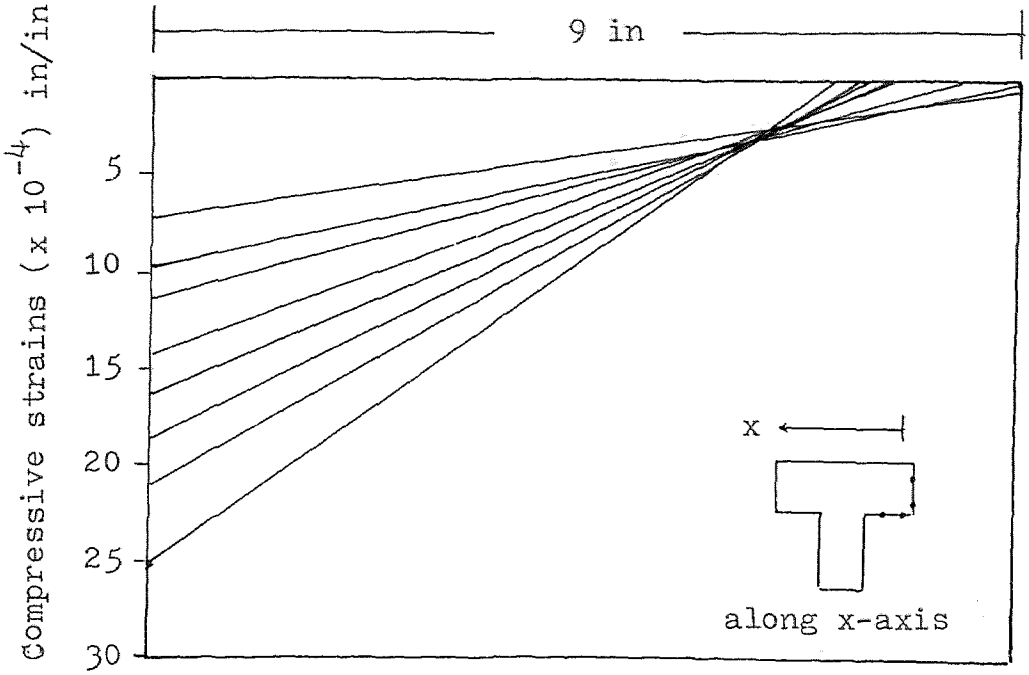

Strains distribution across the flange

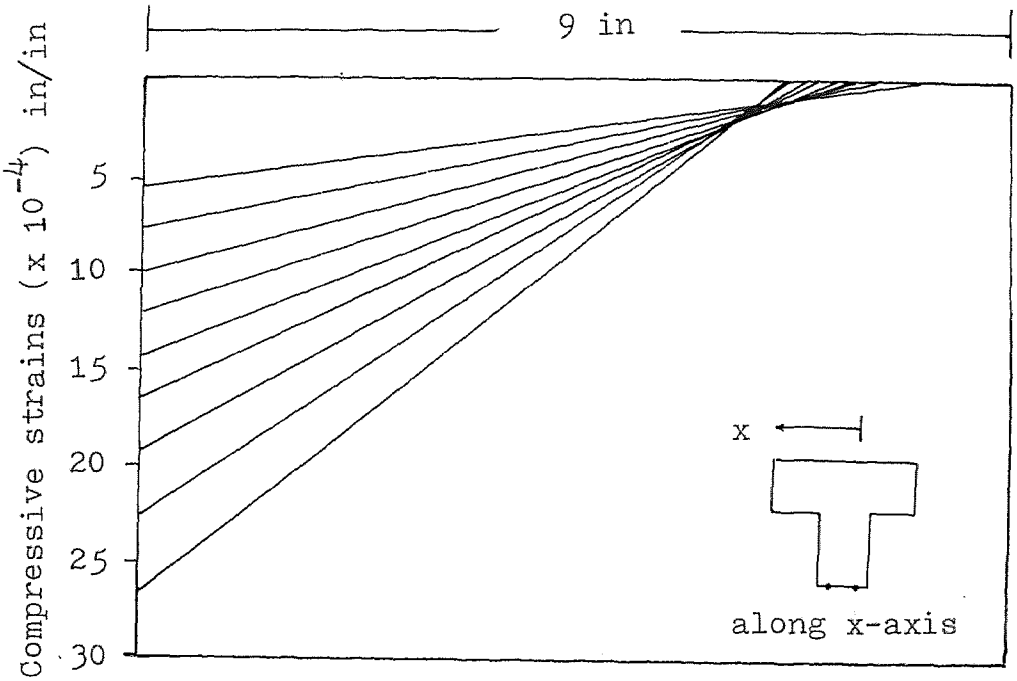

Strain distribution across the web

Figure A-4b Strain distribution across the section for specimen T-6

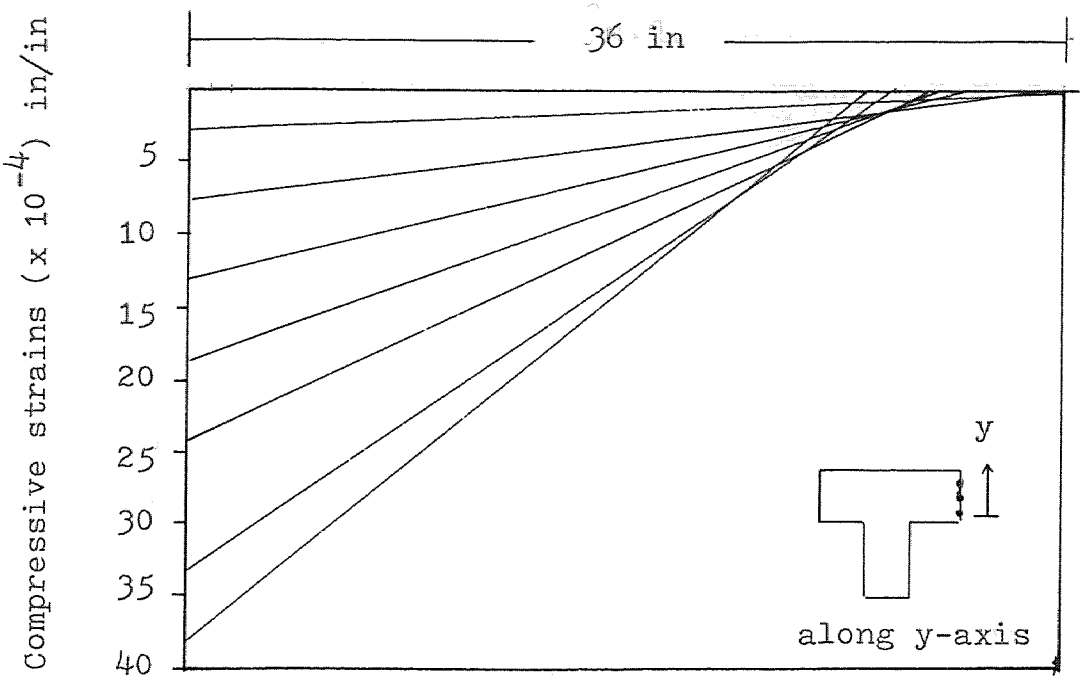

Strain distribution across the flange

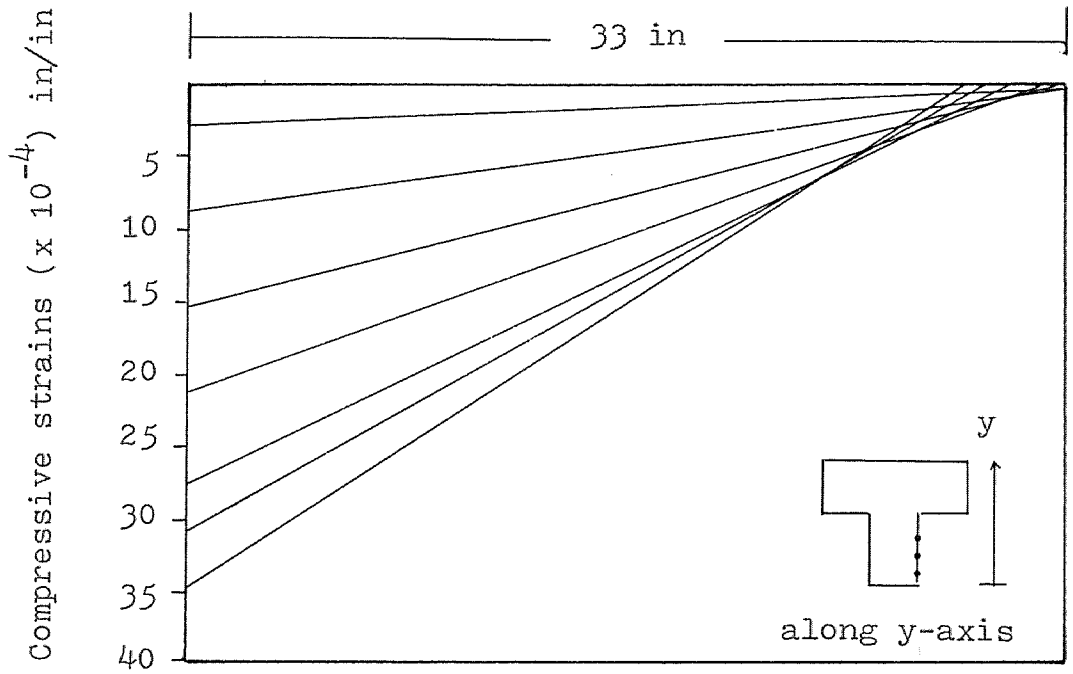

Strain distribution across the web

Figure A-5a Strain distribution across the section for specimen T-6

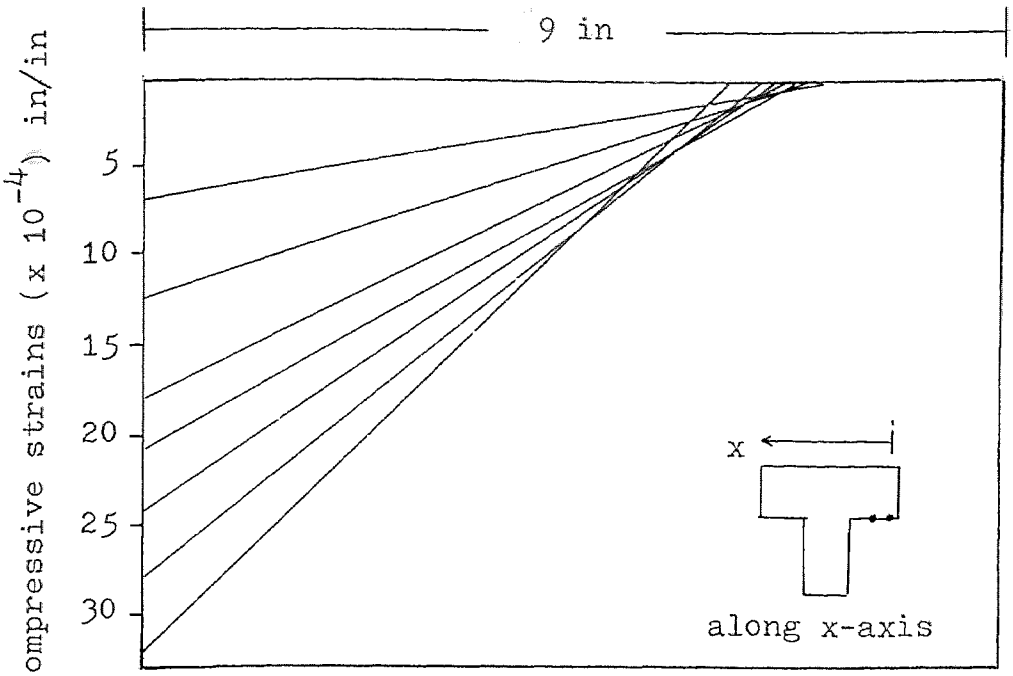

Strain distribution across the flange

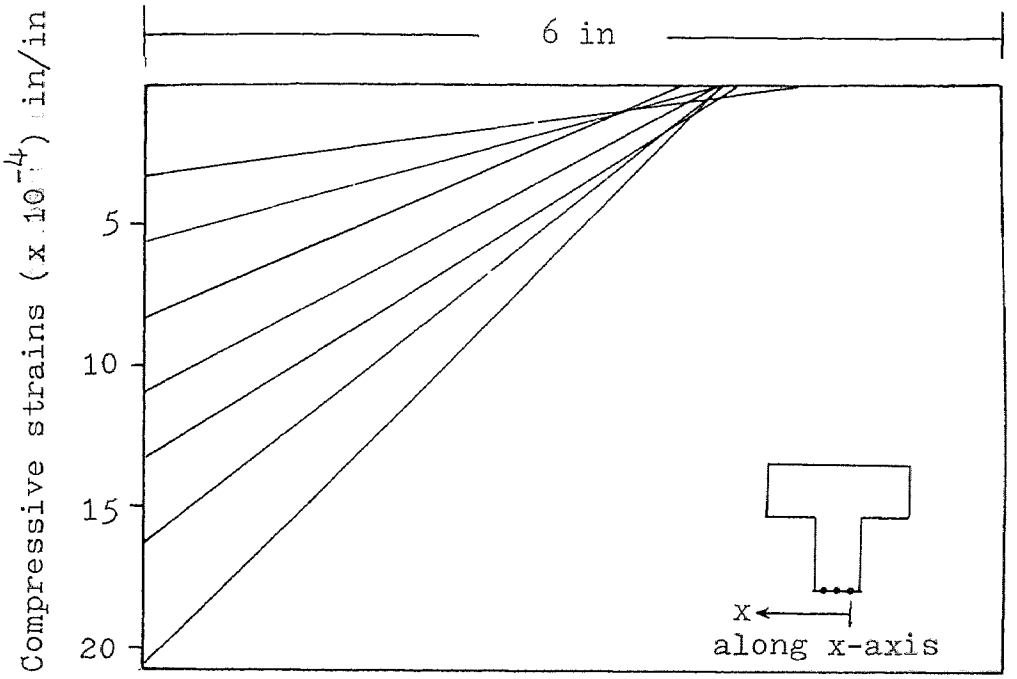

Strain distribution across the web

Figure A-5b Strain distribution across the section for specimen T-6

Table A-6 Load-deflection results for specimen T-1

Loads	Experimental		Theoretical	
	δ_x	δ_y	δ_{2x}	δ_{2y}
kips	inch		inch	
43.51	0.070	0.070	0.081	0.085
52.74	0.096	0.100	0.101	0.107
70.68	0.153	0.166	0.143	0.154
79.24	0.190	0.206	0.167	0.187
87.03	0.233	0.263	0.203	0.244
90.00	0.266	0.303	0.366 F	0.610 F
102.00	0.330	0.400		
108.30	0.373*	0.500*		

*obtained by extrapolation
F denotes failure

Table A-7 Load-deflection results for specimen T-2

Loads	Experimental δ_x	δ_y	Theoretical δ_{2x}	δ_{2y}
kips	inch		inch	
19.83	0.096	0.040	0.120	0.040
24.73	0.128	0.051	0.154	0.050
29.60	0.168	0.068	0.192	0.063
34.57	0.212	0.093	0.249	0.082
39.13	0.280	0.128	0.388	0.120
41.72	0.336	0.160	0.797 F	0.226 F
45.00	0.440	0.200		
48.48	0.720*	0.256*		

*obtained by extrapolation
F denotes failure

Table A-8 Load-deflection results for specimen T-3

Loads	Experimental		Theoretical	
	δ_x	δ_y	δ_{2x}	δ_{2y}
kips	inch		inch	
38.88	0.056	0.064	0.060	0.063
48.22	0.072	0.084	0.077	0.081
57.40	0.092	0.100	0.093	0.099
75.40	0.124	0.140	0.129	0.139
83.83	0.144	0.164	0.149	0.165
92.08	0.164	0.188	0.171	0.197
99.00	0.180	0.210	0.321 F	0.550 F
130.00	0.338	0.376		
139.25	0.408*	0.480*		

*obtained by extrapolation
F denotes failure

Table A-9 Load-deflection results for specimen T-4

Loads	Experimental δ_x	Experimental δ_y	Theoretical δ_{2x}	Theoretical δ_{2y}
kips	inch		inch	
29.44	0.036	0.036	0.044	0.044
38.98	0.053	0.053	0.060	0.060
48.39	0.063	0.066	0.077	0.077
57.65	0.076	0.083	0.095	0.095
66.76	0.093	0.103	0.112	0.114
75.71	0.110	0.126	0.131	0.134
84.50	0.130	0.150	0.150	0.154
92.95	0.156	0.176	0.173	0.182
100.93	0.186	0.213	0.202	0.219
107.00	0.210	0.250	0.366 F	0.550 F
111.50	0.226	0.290		
118.64	0.383*	0.500*		

*obtained by extrapolation

F denotes failure

Table A-10 Load-deflection results for specimen T-6

Loads	Experimental δ_x	Experimental δ_y	Theoretical δ_{2x}	Theoretical δ_{2y}
kips	inch		inch	
29.75	0.053	0.013	0.054	0.014
49.28	0.098	0.026	0.095	0.025
58.94	0.120	0.031	0.117	0.031
68.53	0.141	0.037	0.139	0.037
78.04	0.166	0.044	0.163	0.043
87.47	0.190	0.053	0.188	0.049
96.82	0.220	0.060	0.220	0.053
106.04	0.253	0.070	0.263	0.057
114.71	0.296	0.083	0.351	0.059
118.65	0.316	0.090	0.646 F	0.080 F
122.00	0.366	0.100		
128.94	0.60*	0.110*		

*obtained by extrapolation
F denotes failure

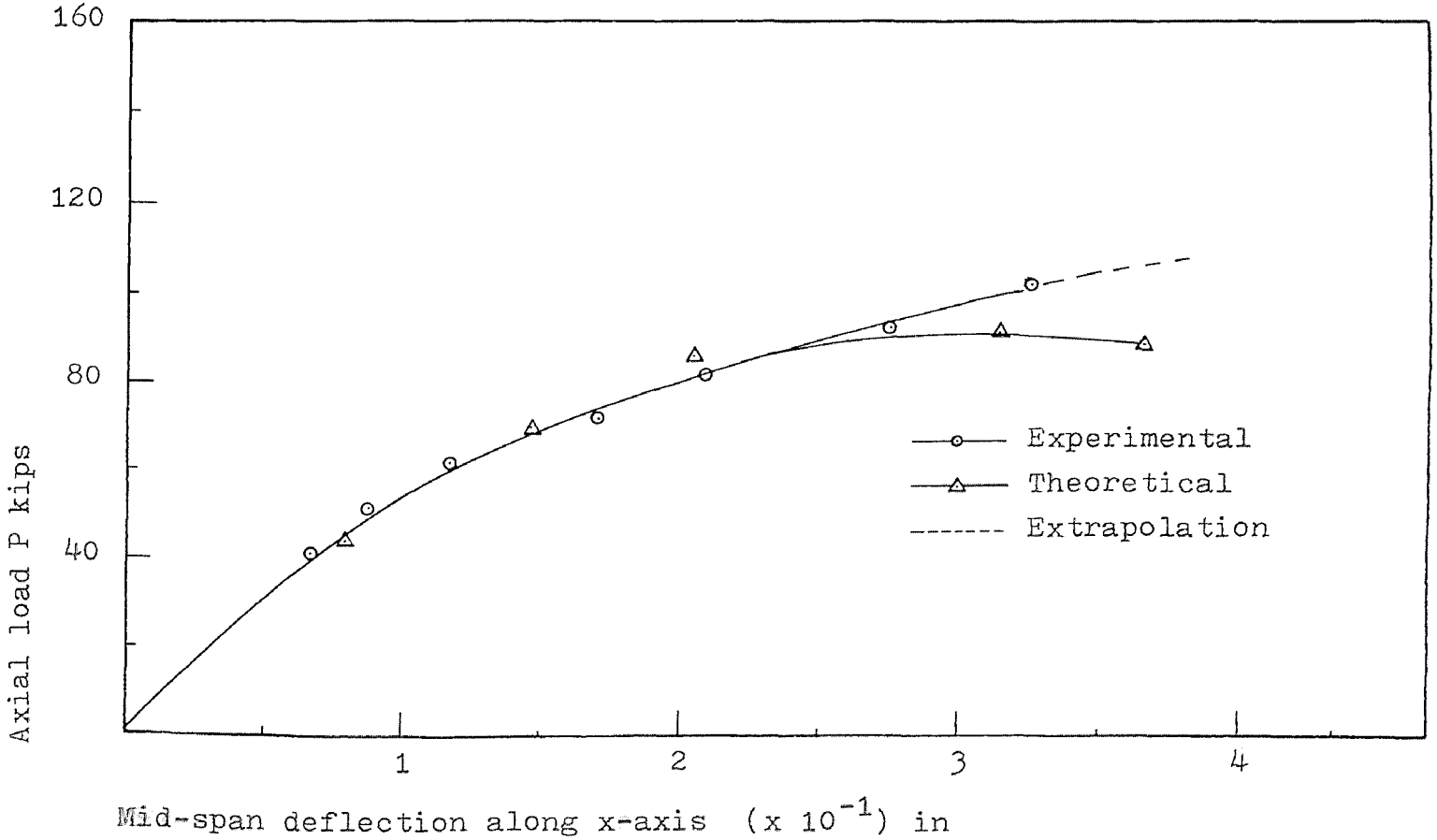

Figure A-6a Load-deflection curves for specimen T-1

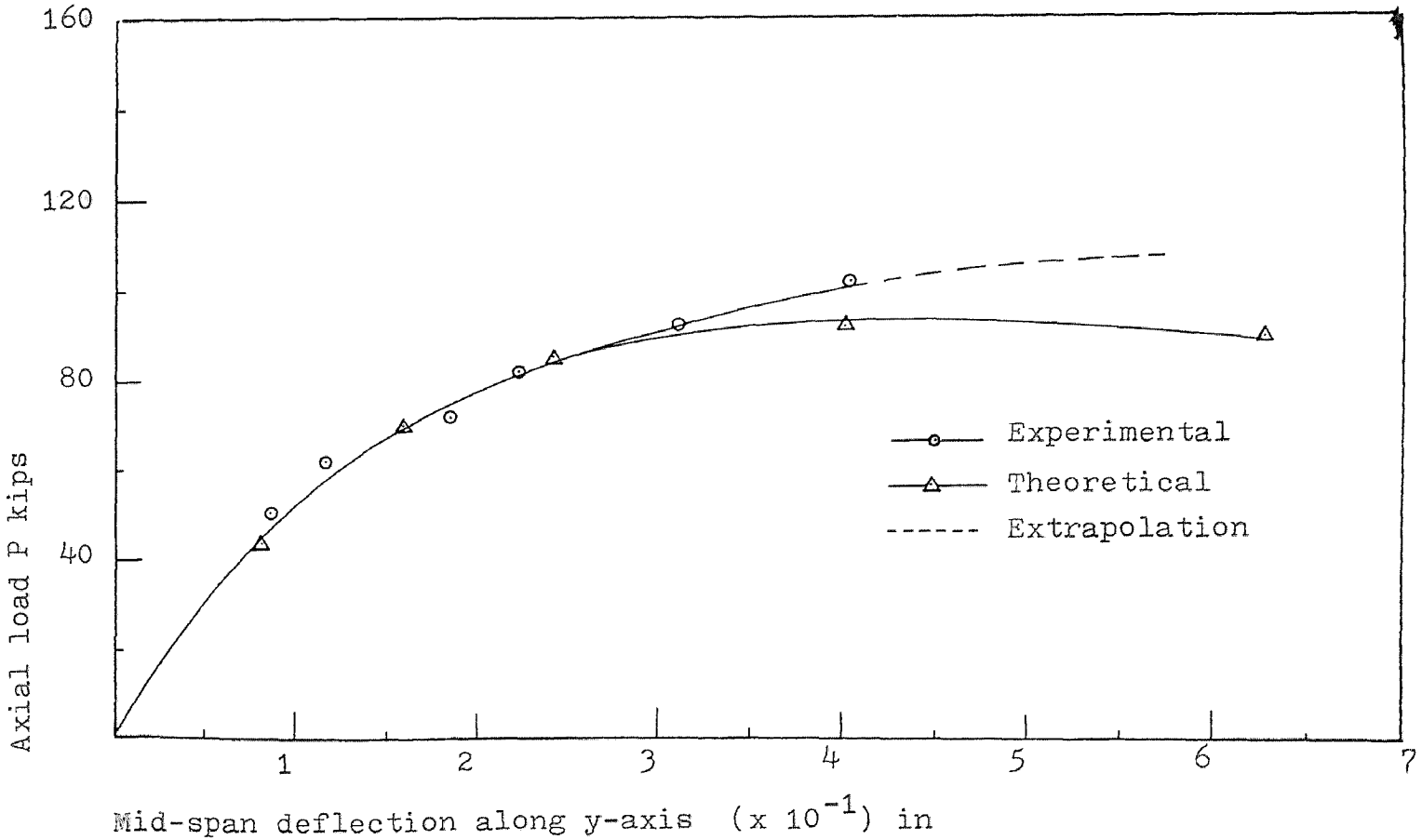

Figure A-6b Load-deflection curves for specimen T-1

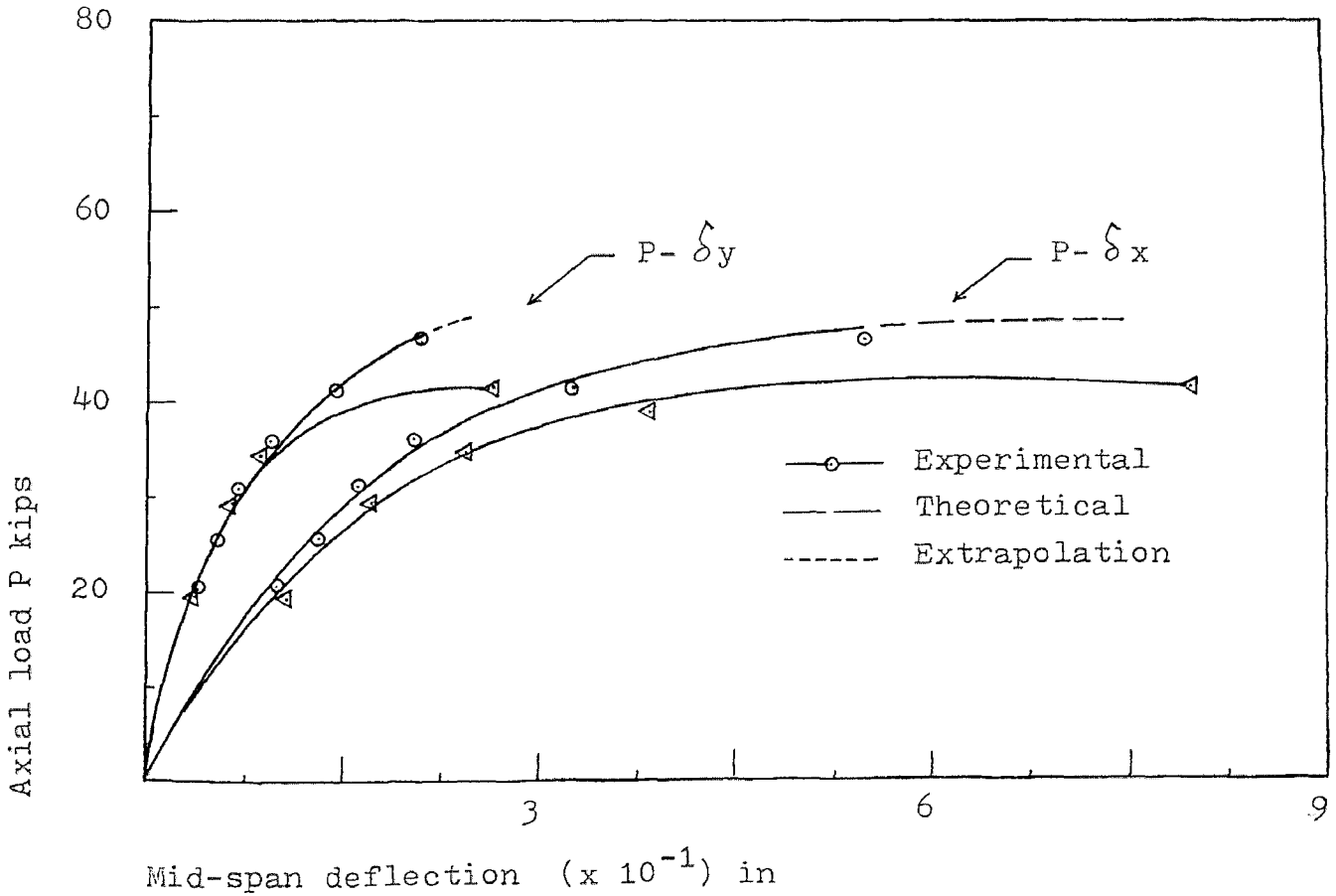

Figure A-7 Load-deflection curves for specimen T-2

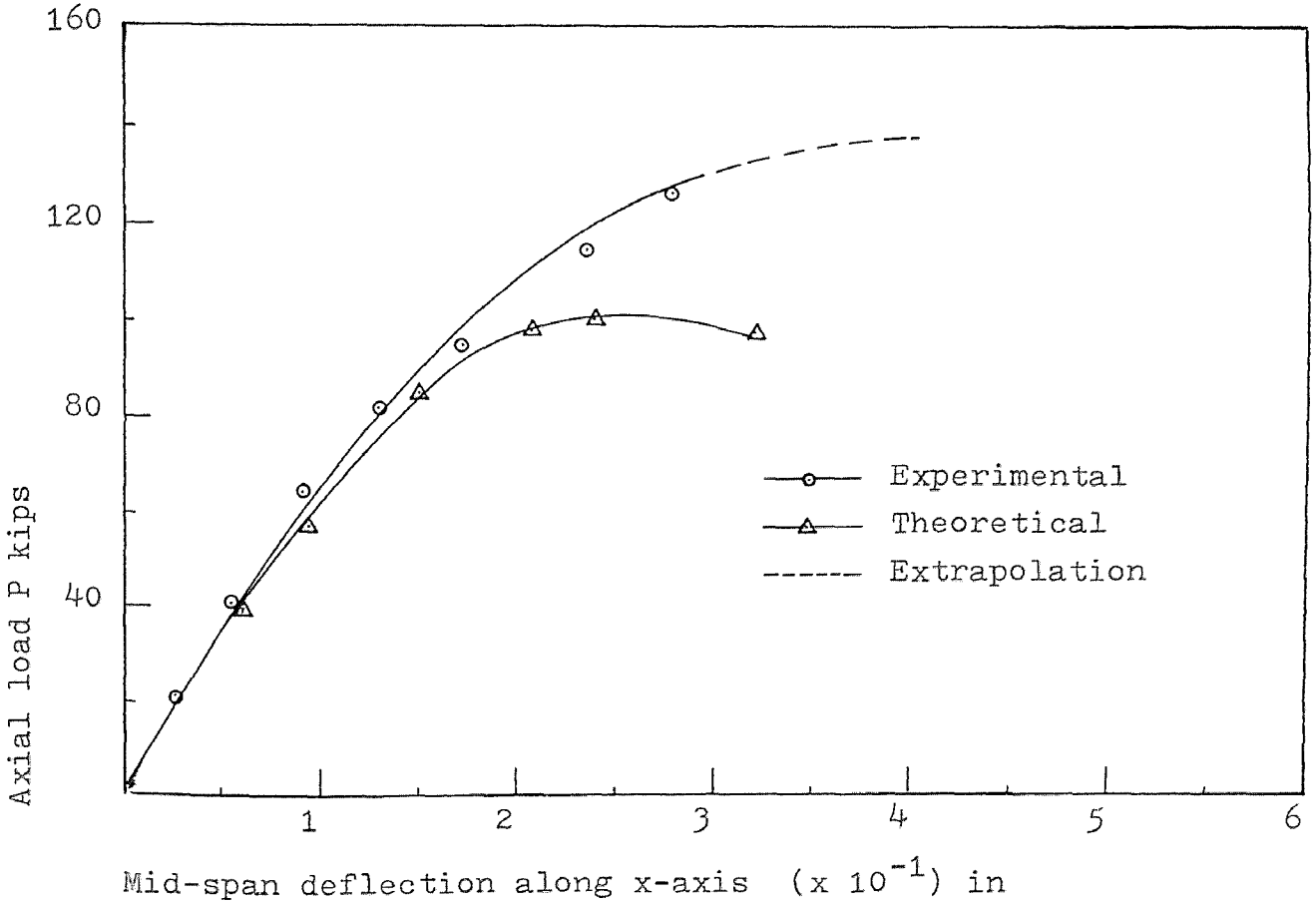

Figure A-8a Load-deflection curves for specimen T-3

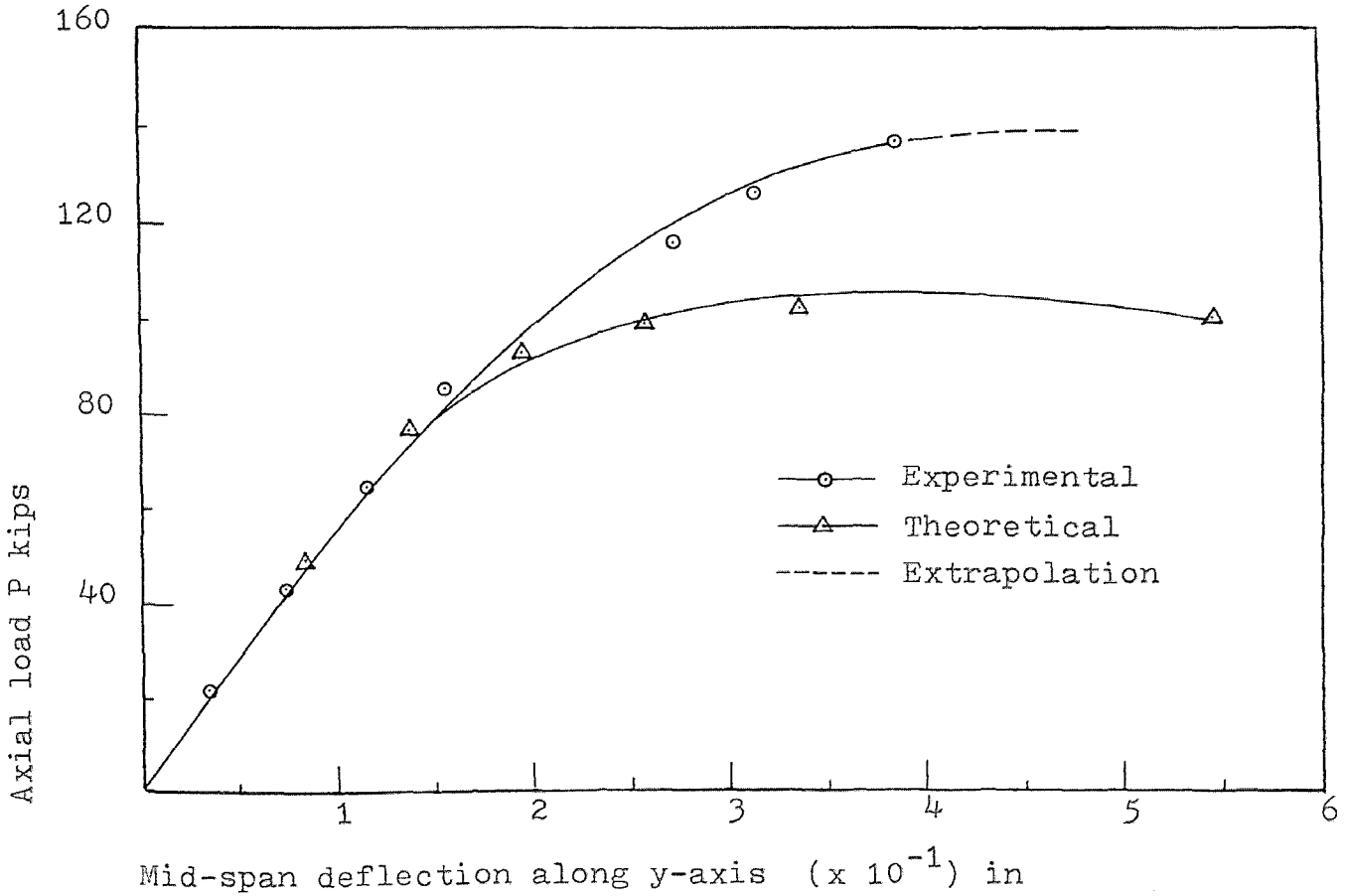

Figure A-8b Load-deflection curves for specimen T-3

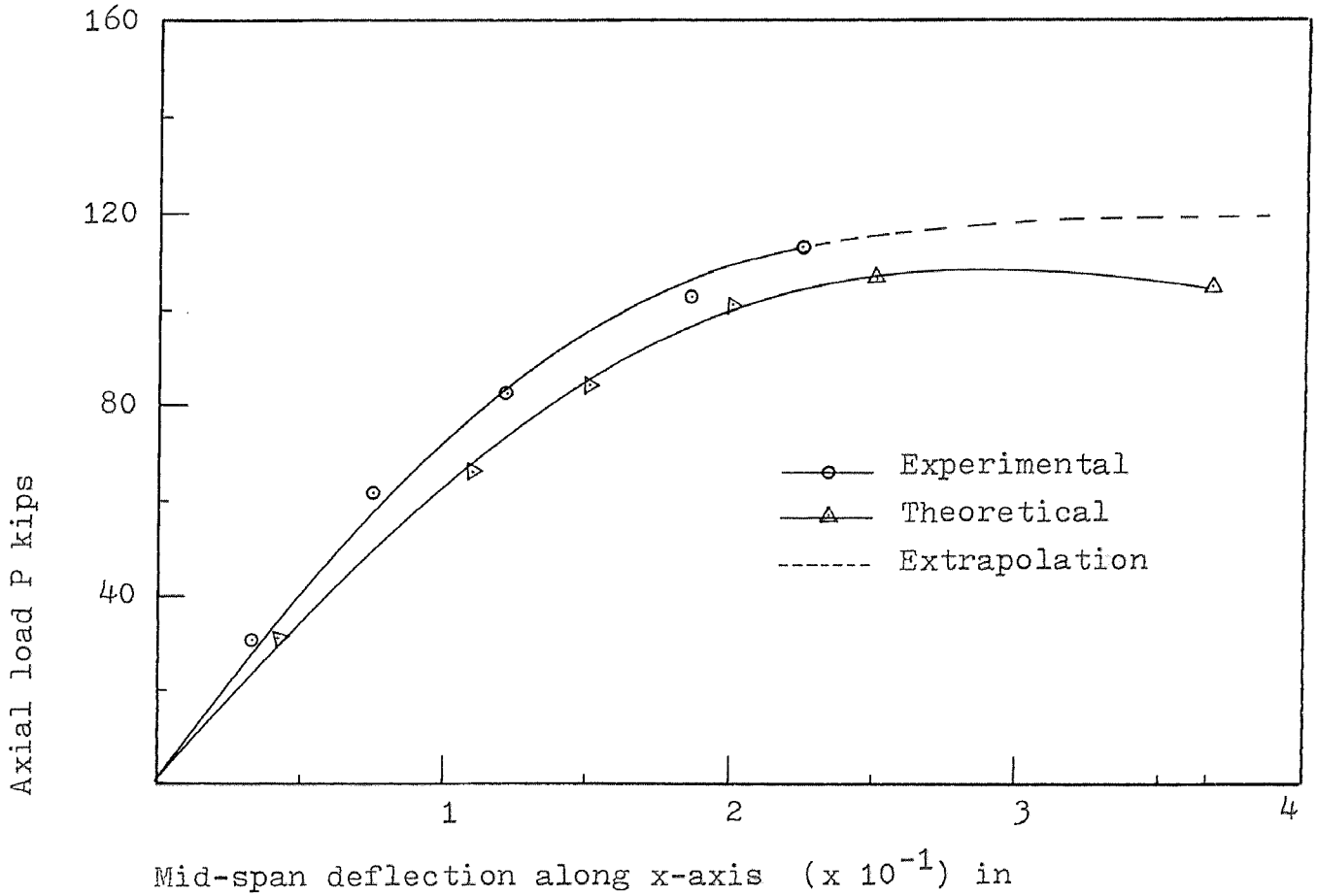

Figure A-9a Load-deflection curves for specimen T-4

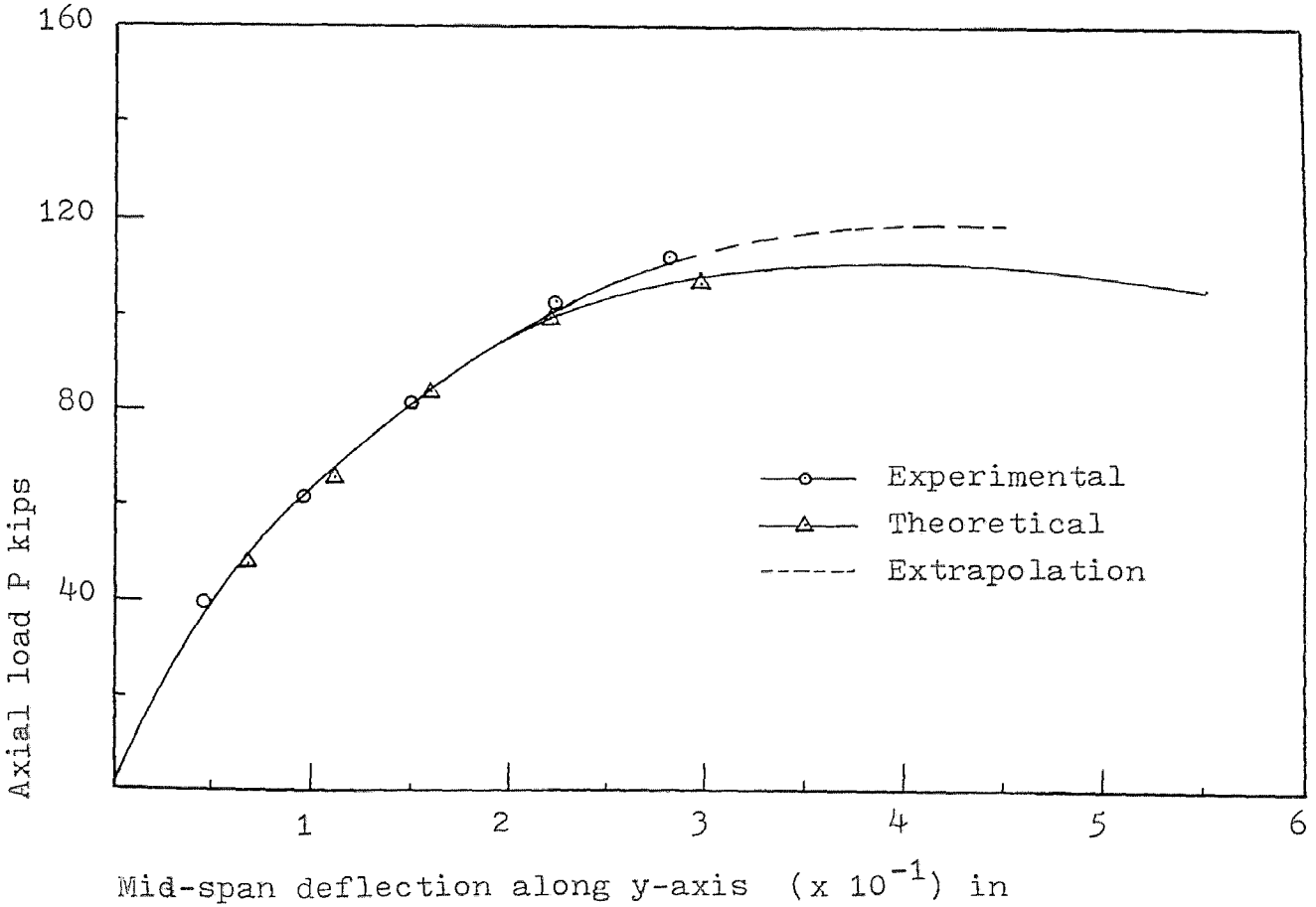

Figure A-9b Load-deflection curves for specimen T-4

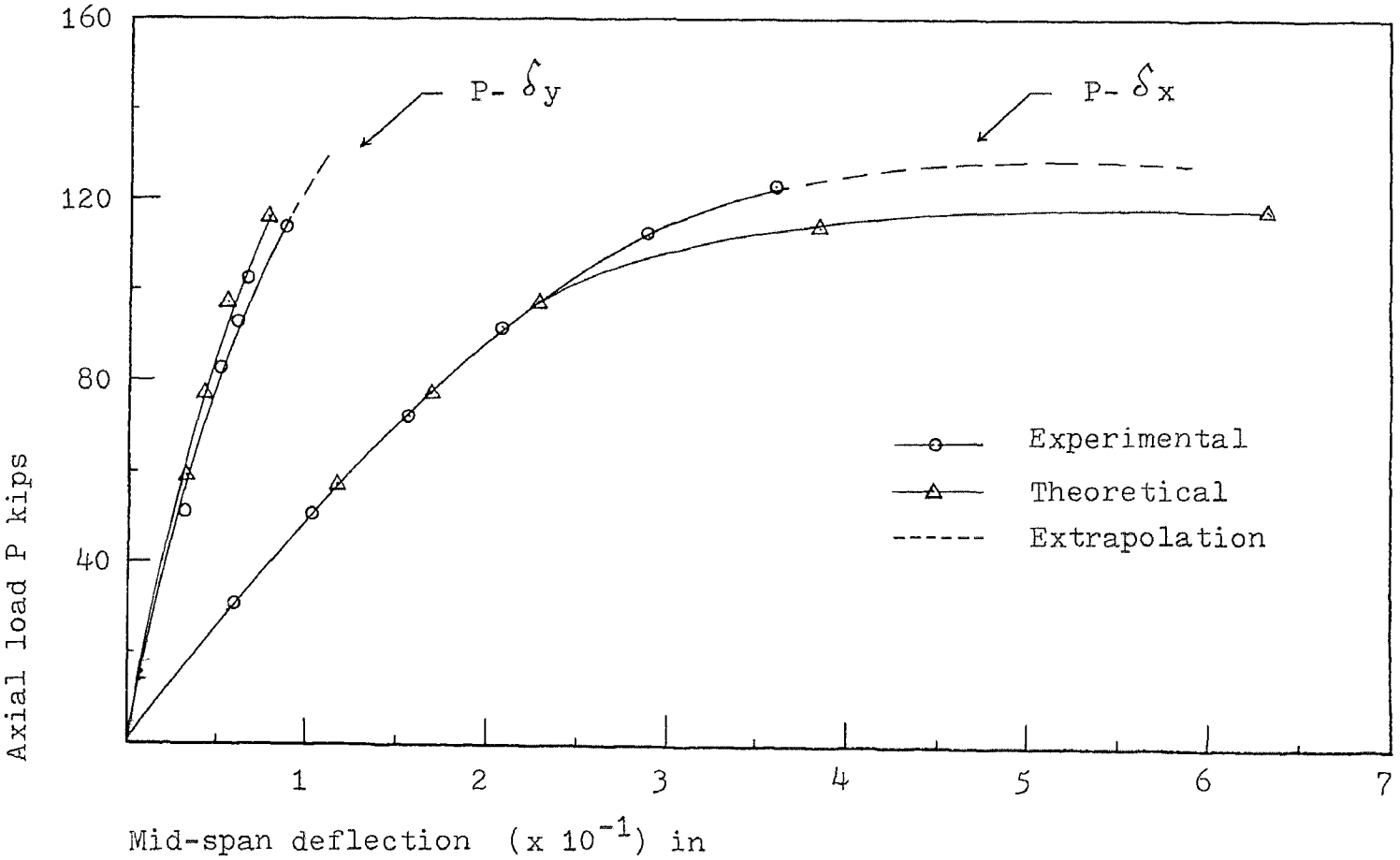

Figure A-10 Load-deflection curves for specimen T-6

Table A-11 Biaxial moment-curvature results for specimen T-1

Experimental					Theoretical				
Loads	Mx	Φx	My	Φy	Loads	Mx	Φx	My	Φy
kips	in-k	1/in	in-k	1/in	kips	in-k	1/in	in-k	1/in
20.63	51.98	---	49.47	29	45.00	112.50	132	106.88	125
30.94	78.46	71	74.72	---	55.00	137.51	166	130.63	157
41.26	105.75	100	100.70	91	65.00	162.51	201	154.38	188
51.57	133.20	137	126.76	---	75.00	187.51	239	178.14	221
61.89	161.90	186	154.41	175	85.00	212.52	289	201.89	259
72.20	192.48	220	182.74	217	95.00	237.52	377	225.64	314
82.52	224.10	276	212.49	270	105.01	262.52	631	249.39	439
92.83	260.20	365	245.16	361	106.92	267.29	960	253.93	566
103.15	299.75	---	278.60	460					
108.30	321.97	---	296.90						

Table A-12 Biaxial moment-curvature results for specimen T-2

Experimental					Theoretical				
Loads	Mx	Φx	My	Φy	Loads	Mx	Φx	My	Φy
kips	in-k	1/in	in-k	1/in	kips	in-k	1/in	in-k	1/in
20.63	31.77	---	155.50	194	20.00	30.00	62	148.76	186
25.78	40.01	74	195.07	246	25.00	37.50	78	185.95	238
30.94	48.57	98	235.05	313	30.00	45.00	98	223.14	297
36.10	57.47	125	275.87	424	35.18	52.77	127	261.62	385
41.26	67.87	201	320.26	641	40.18	60.27	186	298.82	600
46.41	79.68	291	370.67	1090	44.00	65.98	349	327.16	1230
48.48	84.84	---	395.45	----					

Table A-13 Biaxial moment-curvature results for specimen T-3

Experimental					Theoretical				
Loads	Mx	Φx	My	Φy	Loads	Mx	Φx	My	Φy
kips	in-k	1/in	in-k	1/in	kips	in-k	1/in	in-k	1/in
20.63	43.81	44	43.77	---	40.00	87.50	98	83.75	93
30.94	69.20	70	66.21	72	50.00	109.38	125	104.69	119
41.26	92.96	100	88.79	107	-----	------	---	------	---
51.57	117.00	124	111.60	150	75.00	164.06	200	157.03	186
61.89	141.72	156	135.40	169	80.00	175.00	216	167.50	200
72.20	166.80	189	158.84	189	90.00	196.88	256	188.44	231
82.52	192.30	236	182.53	234	100.00	218.76	305	209.38	264
92.38	218.40	271	209.79	264	110.00	240.64	411	230.32	322
103.15	245.50	325	234.76	298	115.00	251.58	516	240.79	369
113.46	273.10	---	261.86	366	118.92	260.44	849	248.99	496
123.78	303.30	593	289.60	449					
134.10	339.30	---	323.98	608					
139.25	375.55	---	337.80	---					

Table A-14 Biaxial moment-curvature results for specimen T-4

Experimental					Theoretical				
Loads	Mx	Φx	My	Φy	Loads	Mx	Φx	My	Φy
kips	in-k	1/in	in-k	1/in	kips	in-k	1/in	in-k	1/in
20.63	49.30	---	48.00	---	30.00	71.25	68	69.37	68
30.94	74.60	65	72.30	71	40.00	95.00	94	92.50	94
41.26	100.00	---	97.00	96	50.00	118.75	120	115.63	120
51.57	125.90	---	121.97	134	60.00	142.50	148	138.75	147
61.89	152.60	145	147.60	162	70.00	166.26	177	161.88	174
72.20	179.80	177	173.60	186	80.00	190.01	207	185.01	203
82.52	207.50	221	200.00	221	90.00	213.76	239	208.14	232
92.83	236.50	269	227.50	262	100.00	237.51	282	231.26	267
103.15	268.70	312	256.30	310	110.00	261.27	339	254.39	312
113.46	302.40	380	287.30	352	120.00	285.02	459	277.52	388
118.62	329.17	---	314.00	---	127.52	302.87	740	294.90	520

Table A-15 Biaxial moment-curvature results for specimen T-6

Experimental					Theoretical				
Loads	Mx	Φx	My	Φy	Loads	Mx	Φx	My	Φy
kips	in-k	1/in	in-k	1/in	kips	in-k	1/in	in-k	1/in
10.31	5.84	8	31.10	---	30.00	16.80	23	90.00	84
30.94	17.82	22	94.61	82	40.00	22.40	32	120.00	115
51.57	30.43	41	160.02	145	50.00	28.00	40	150.01	148
72.20	43.53	60	227.43	225	60.00	33.60	49	180.02	182
92.83	57.55	80	297.98	315	70.00	39.20	58	210.02	216
103.15	64.98	96	333.48	391	80.00	44.80	67	240.03	253
113.46	72.95	112	372.48	473	90.01	50.40	76	270.03	291
123.78	82.43	136	416.27	630	100.01	56.00	83	300.04	341
128.94	87.68	---	455.54	---	110.01	61.60	88	330.05	406
					120.01	67.21	92	360.05	542
					125.02	70.01	86	375.06	685
					128.07	71.72	101	384.22	998

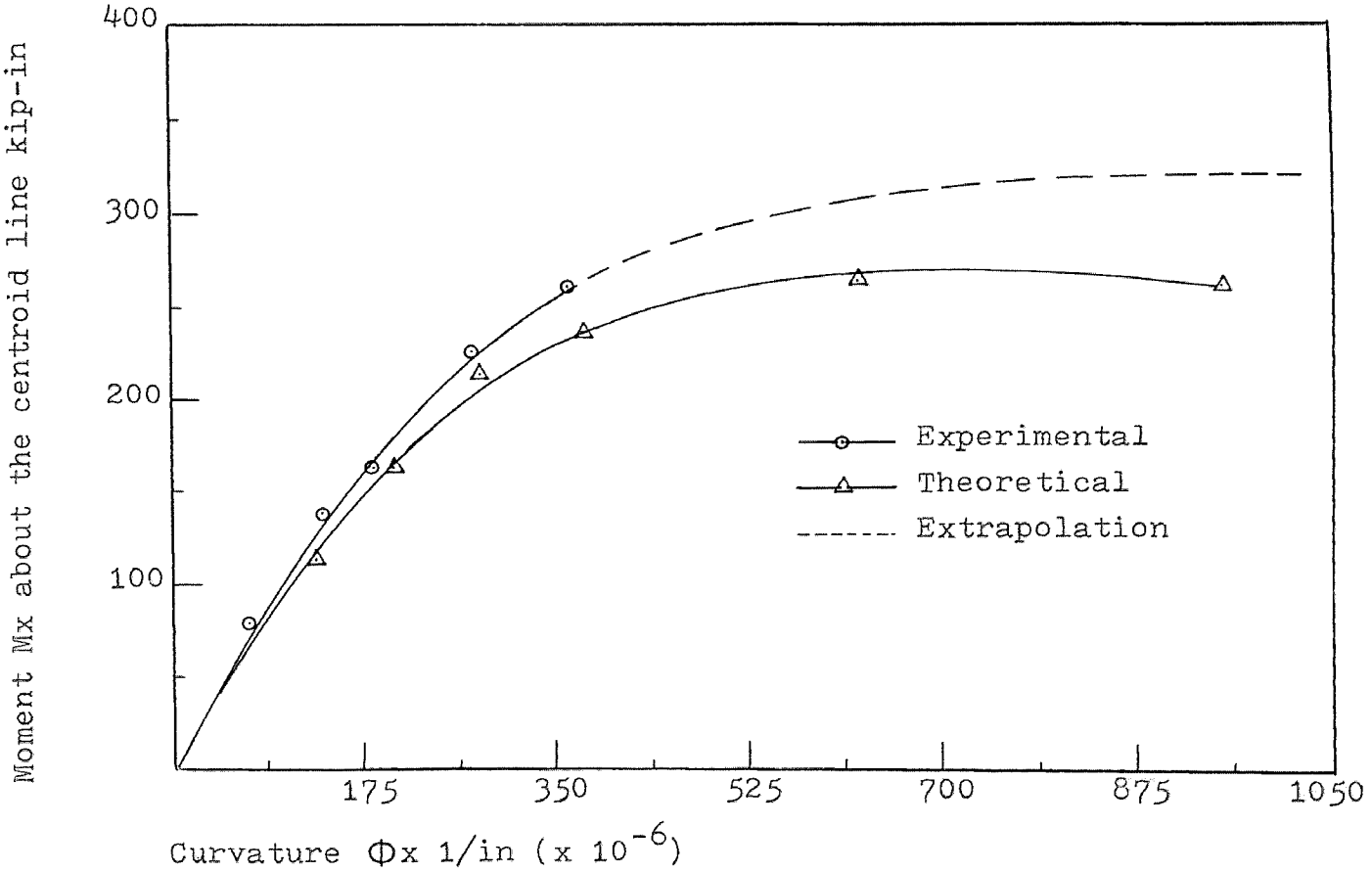

Figure A-11a Biaxial moment-curvature curves for specimen T-1

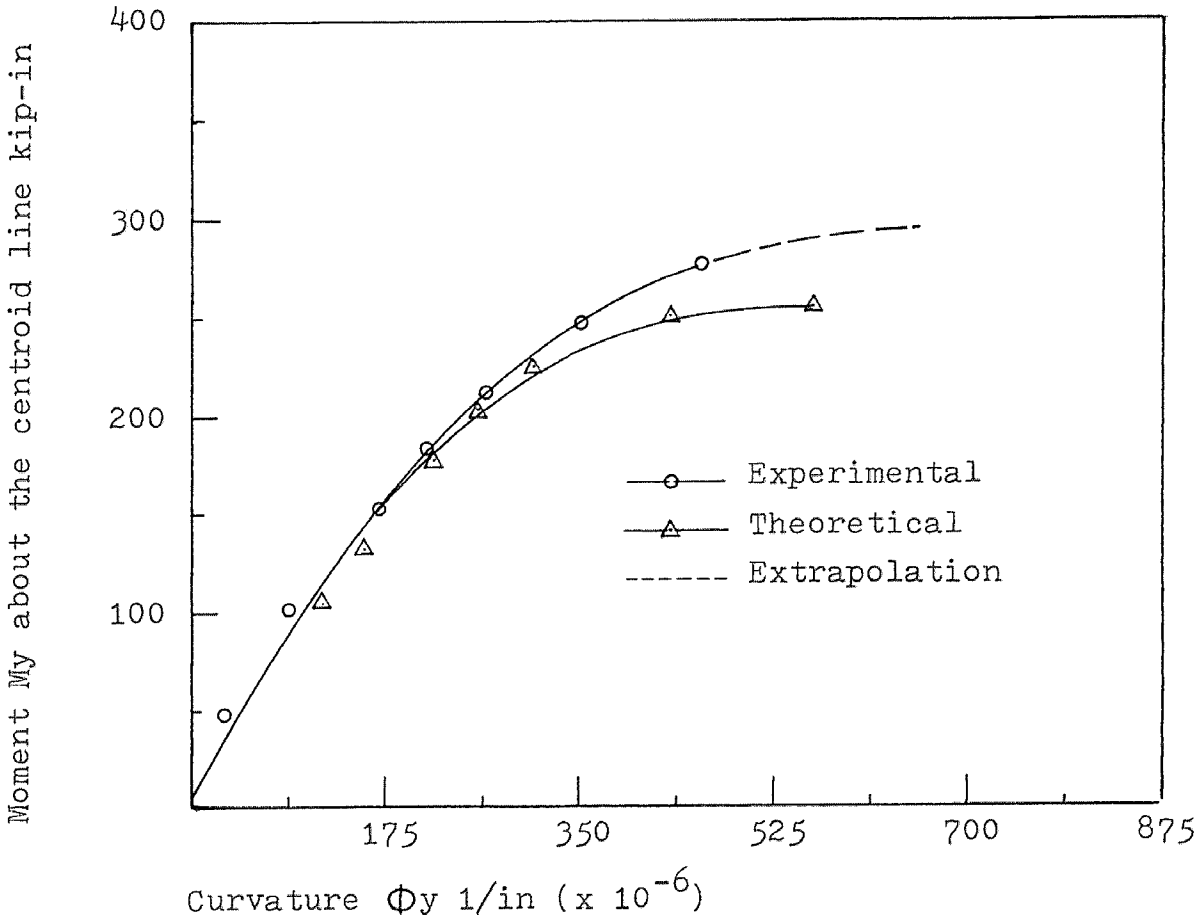

Figure A-11b Biaxial moment-curvature curves for specimen T-1

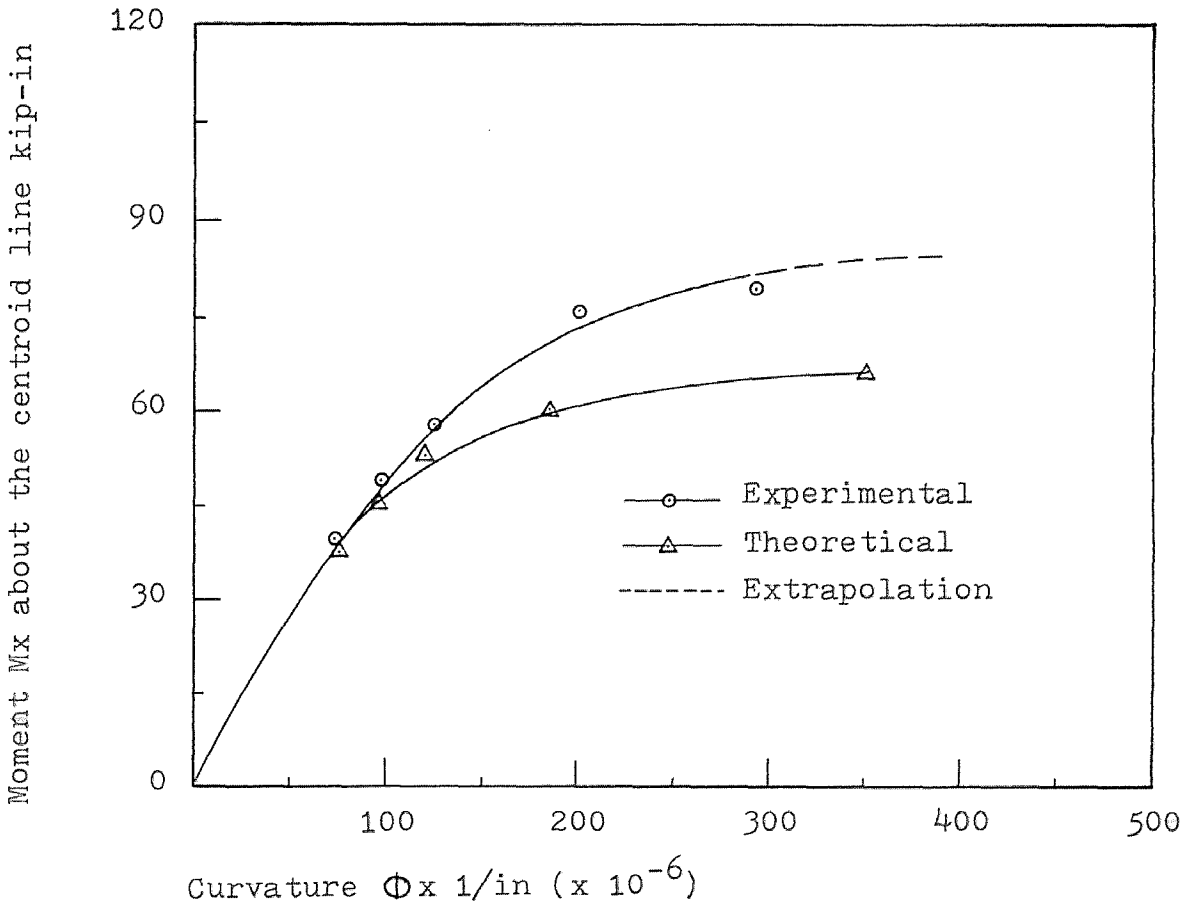

Figure A-12a Biaxial moment-curvature curves for specimen T-2

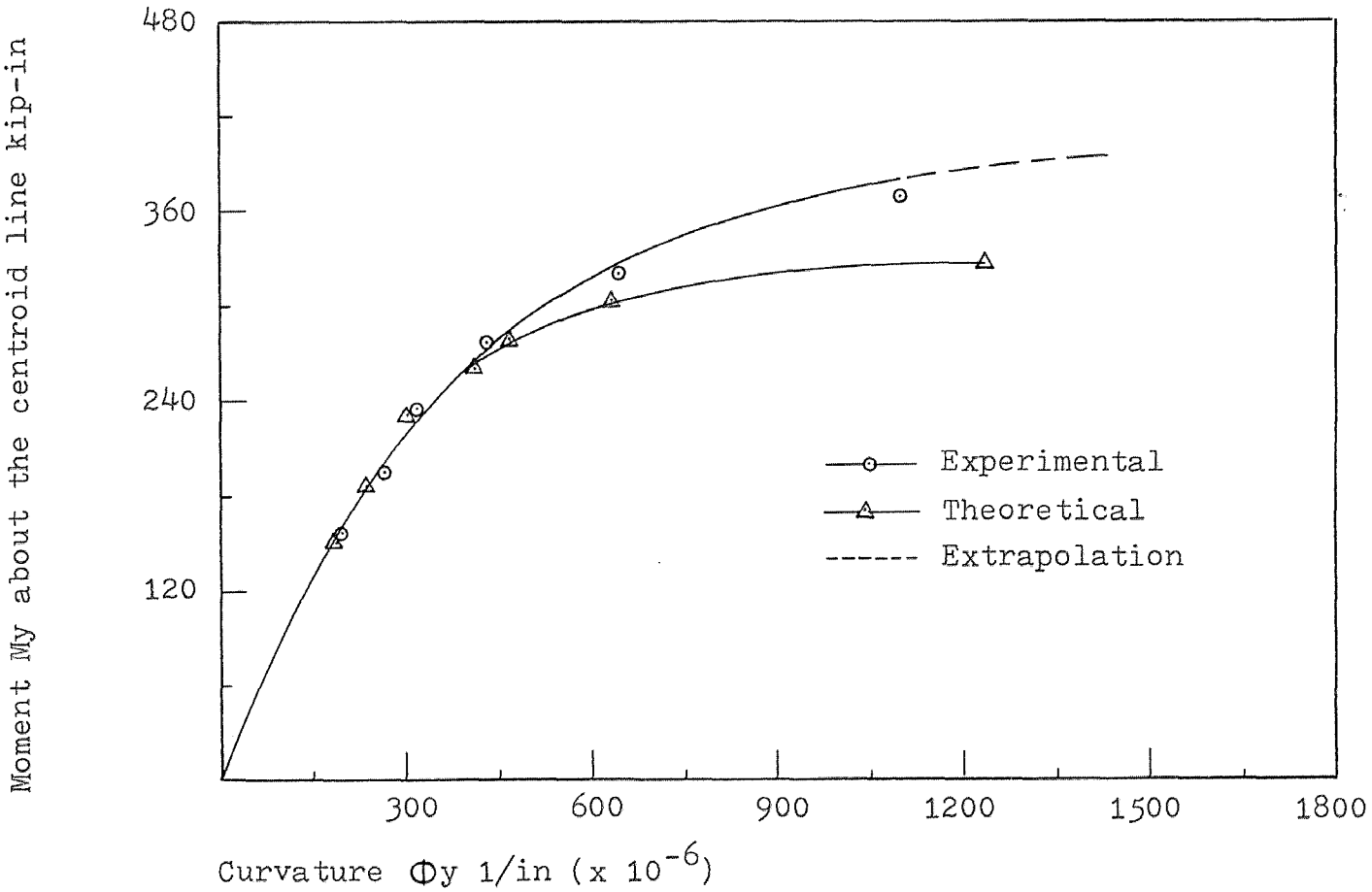

Figure A-12b Biaxial moment-curvature curves for specimen T-2

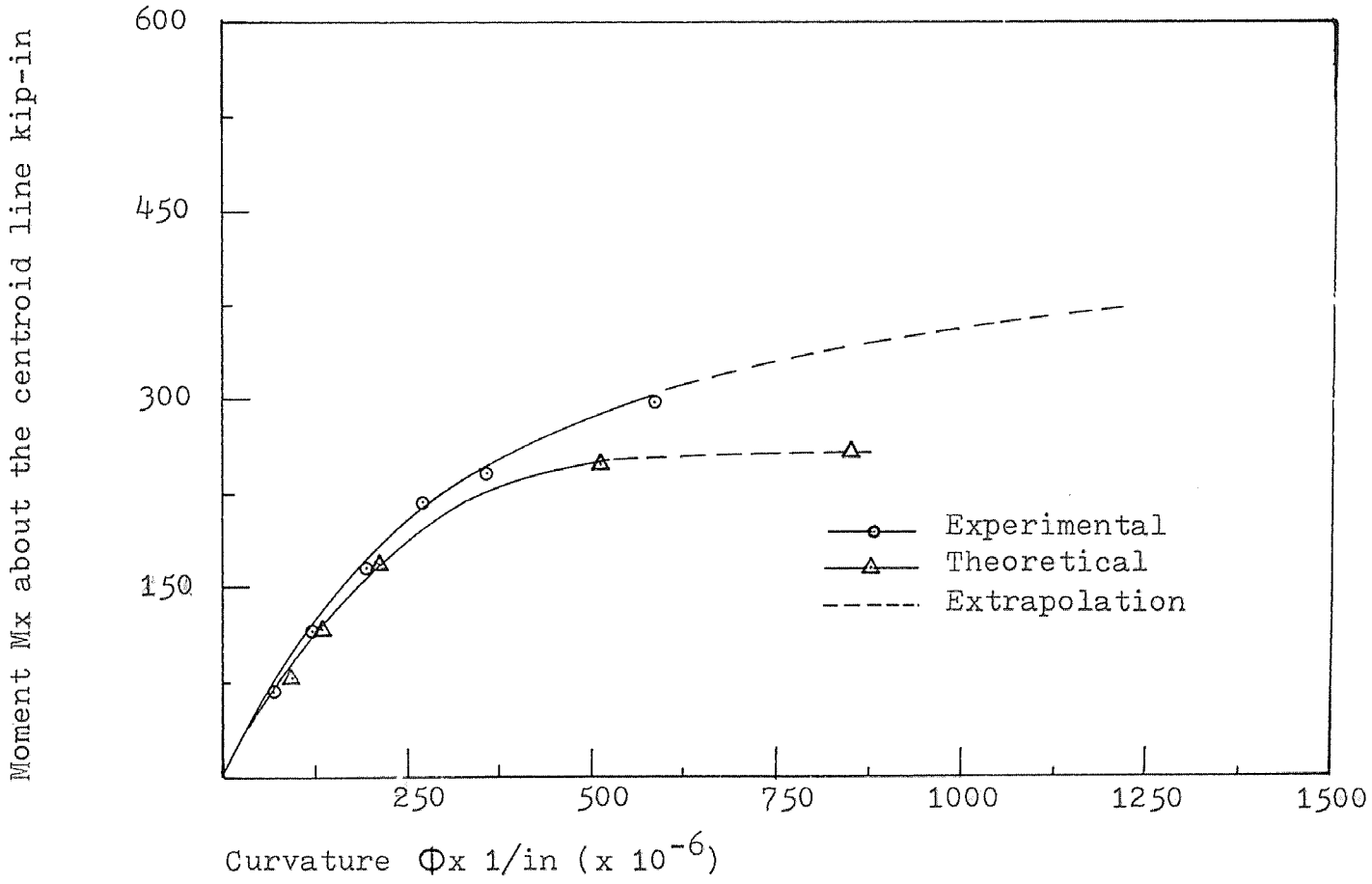

Figure A-13a Biaxial moment-curvature curves for specimen T-3

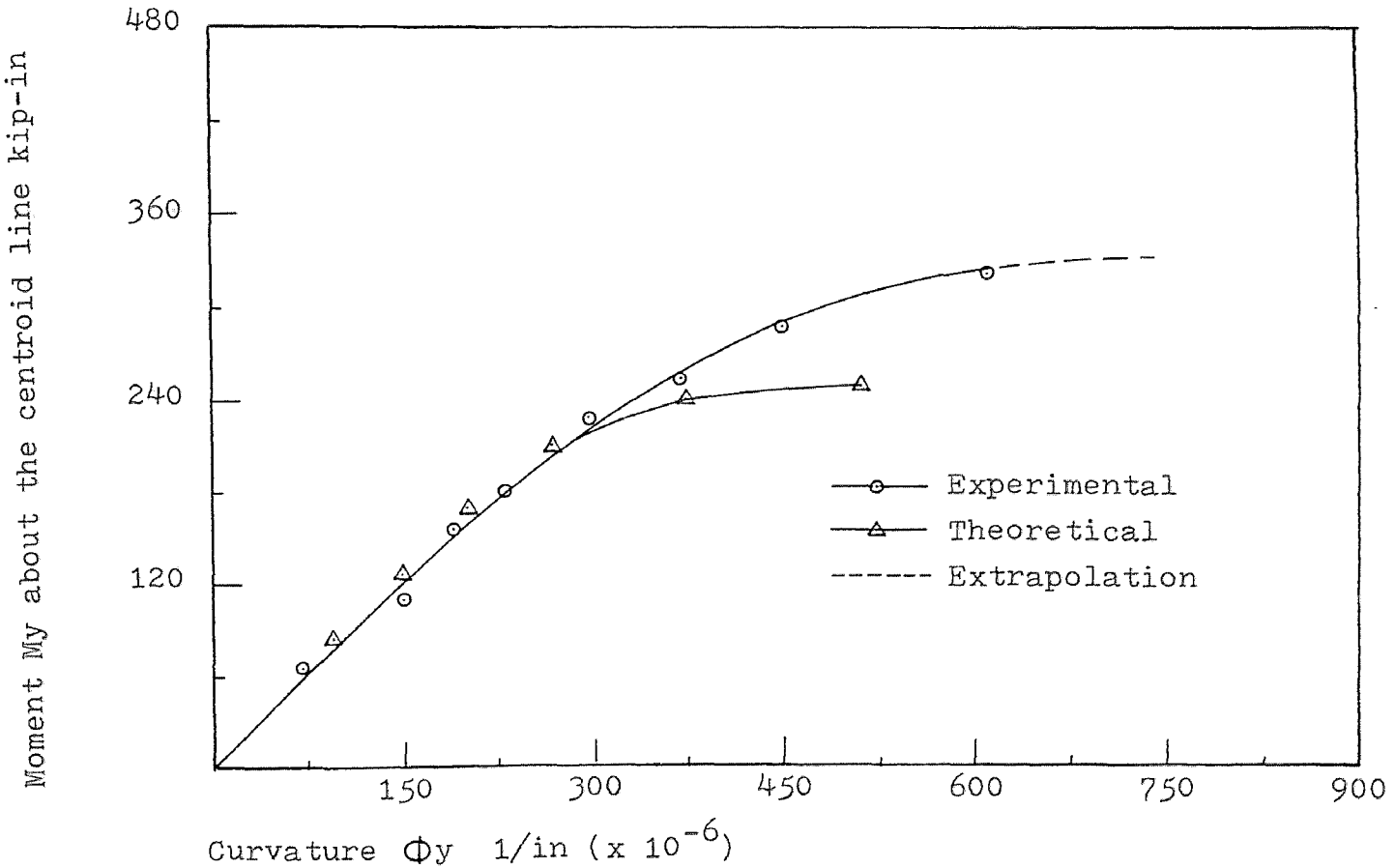

Figure A-13b Biaxial moment-curvature curves for specimen T-3

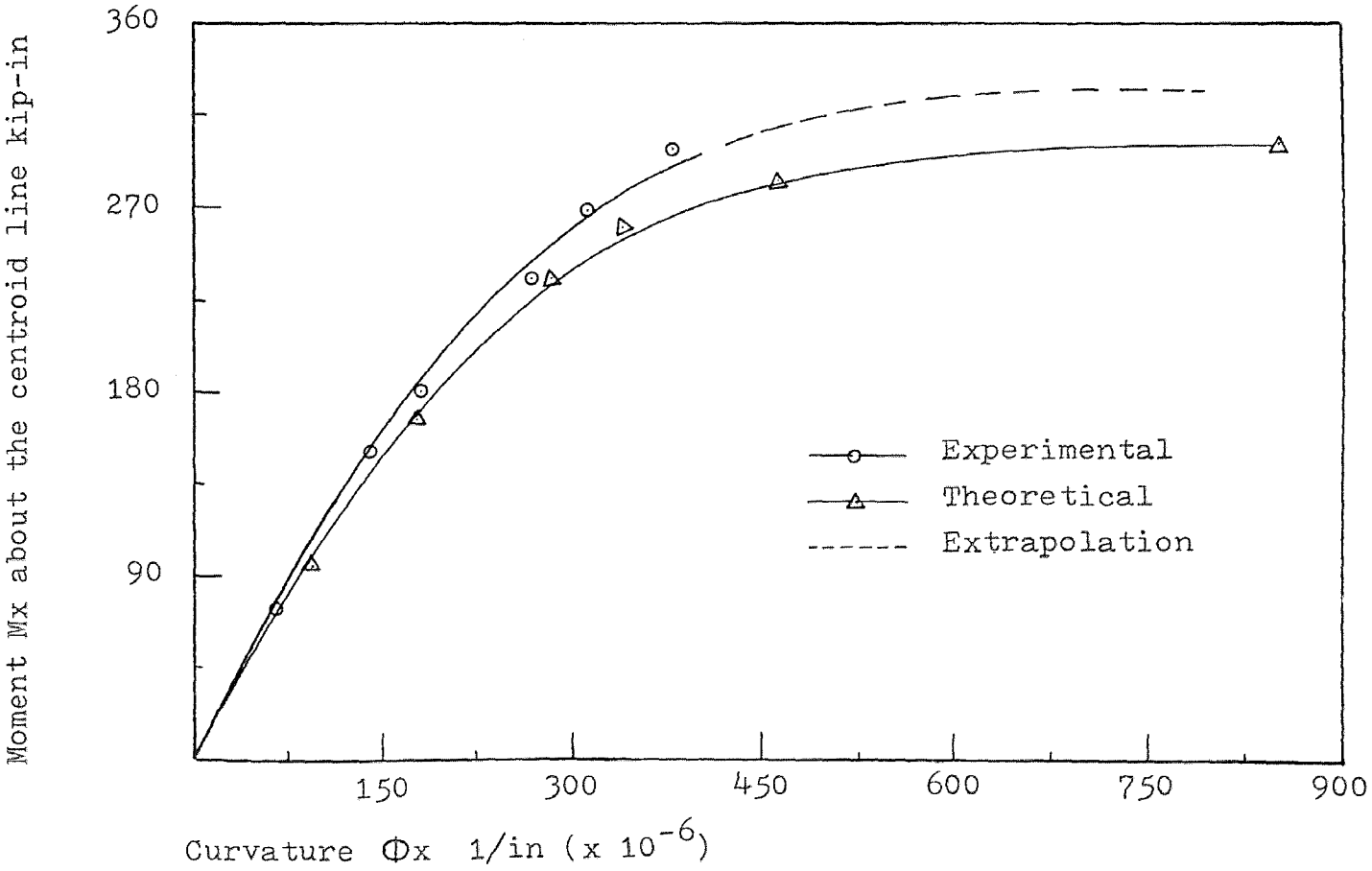

Figure A-14a Biaxial moment-curvature curves for specimen T-4

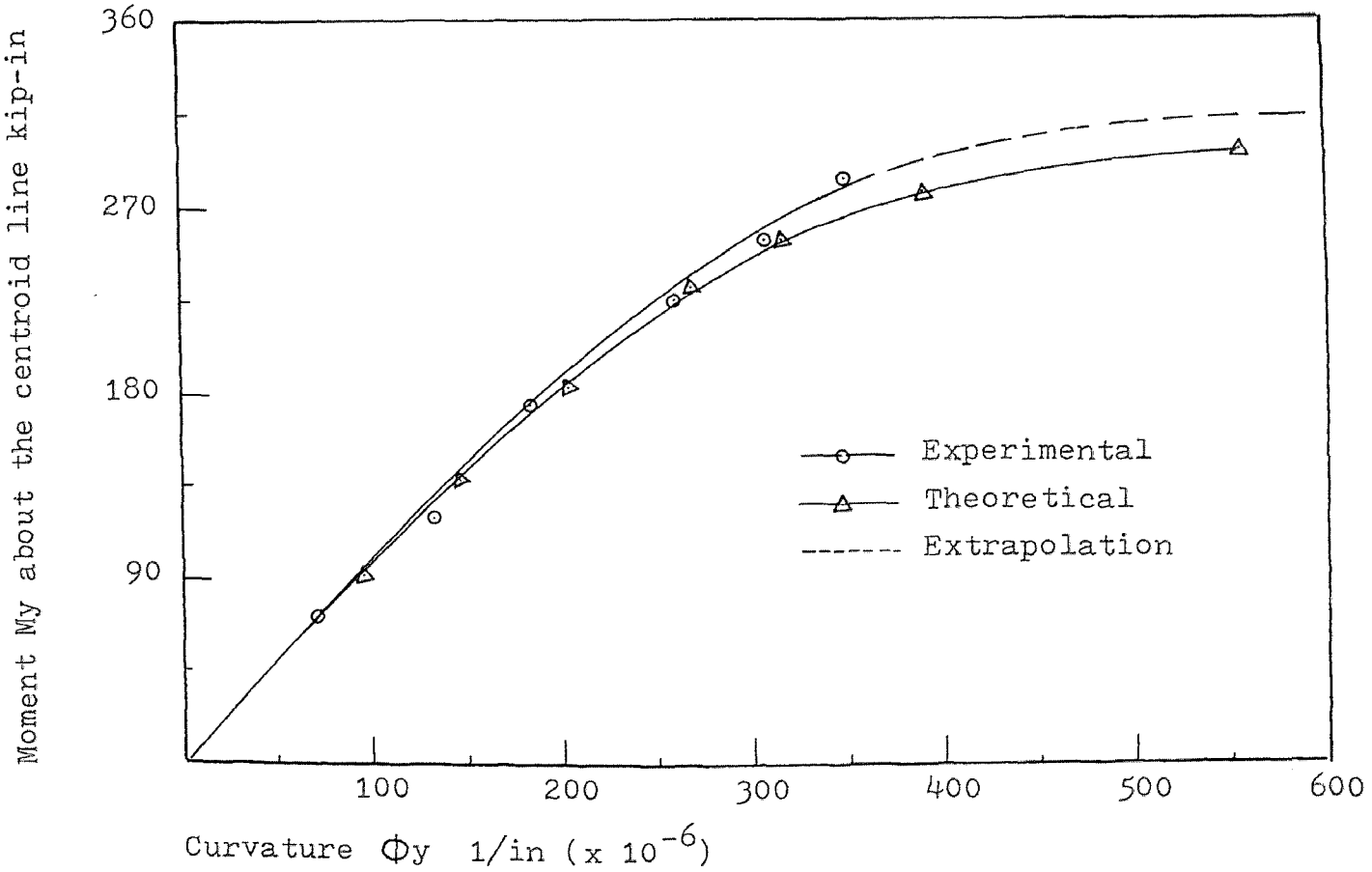

Figure A-14b Biaxial moment-curvature curves for specimen T-4

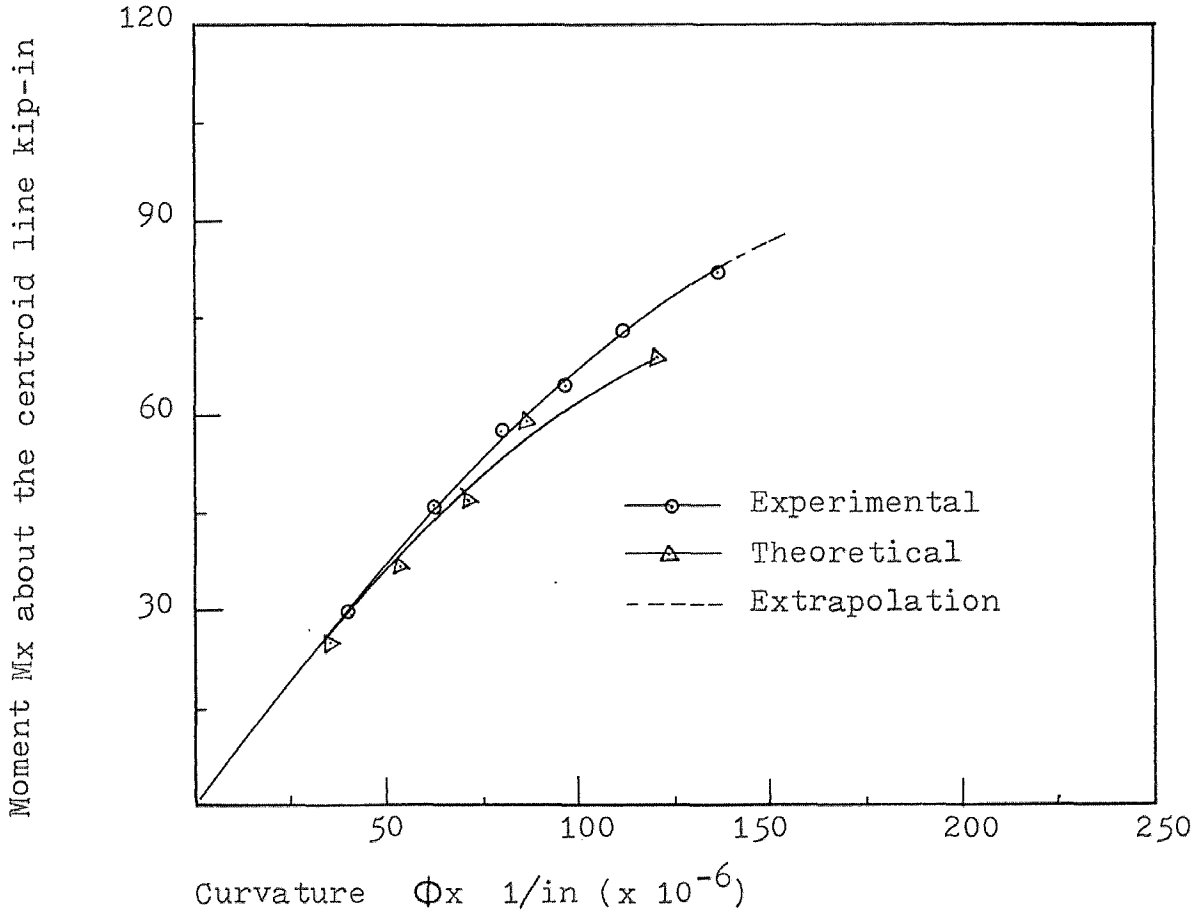

Figure A-15a Biaxial moment-curvature curves for specimen T-6

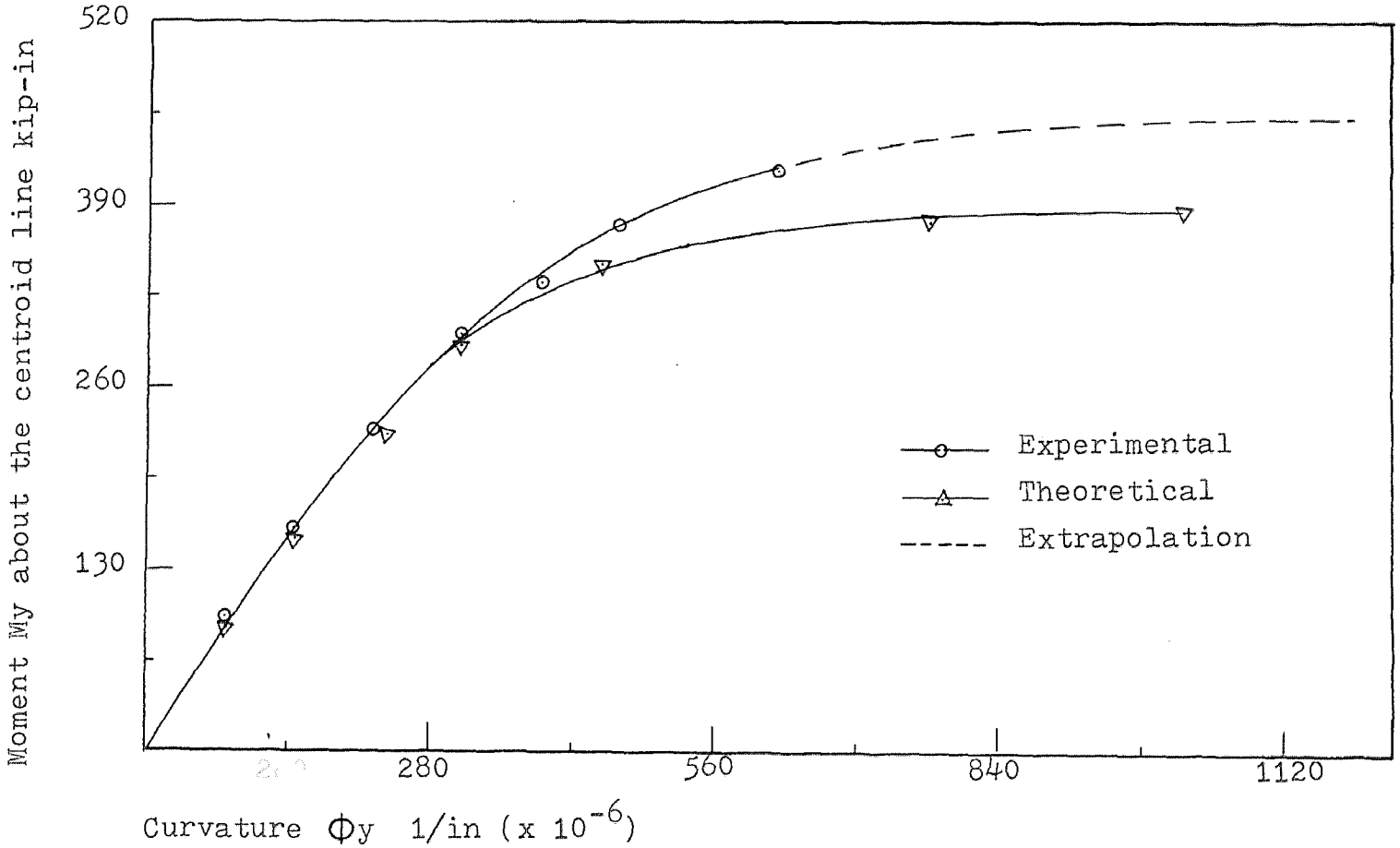

Figure A-15b Biaxial moment-curvature curves for specimen T-6

Appendix B

Element Coordinates and Area for Computer Program Input

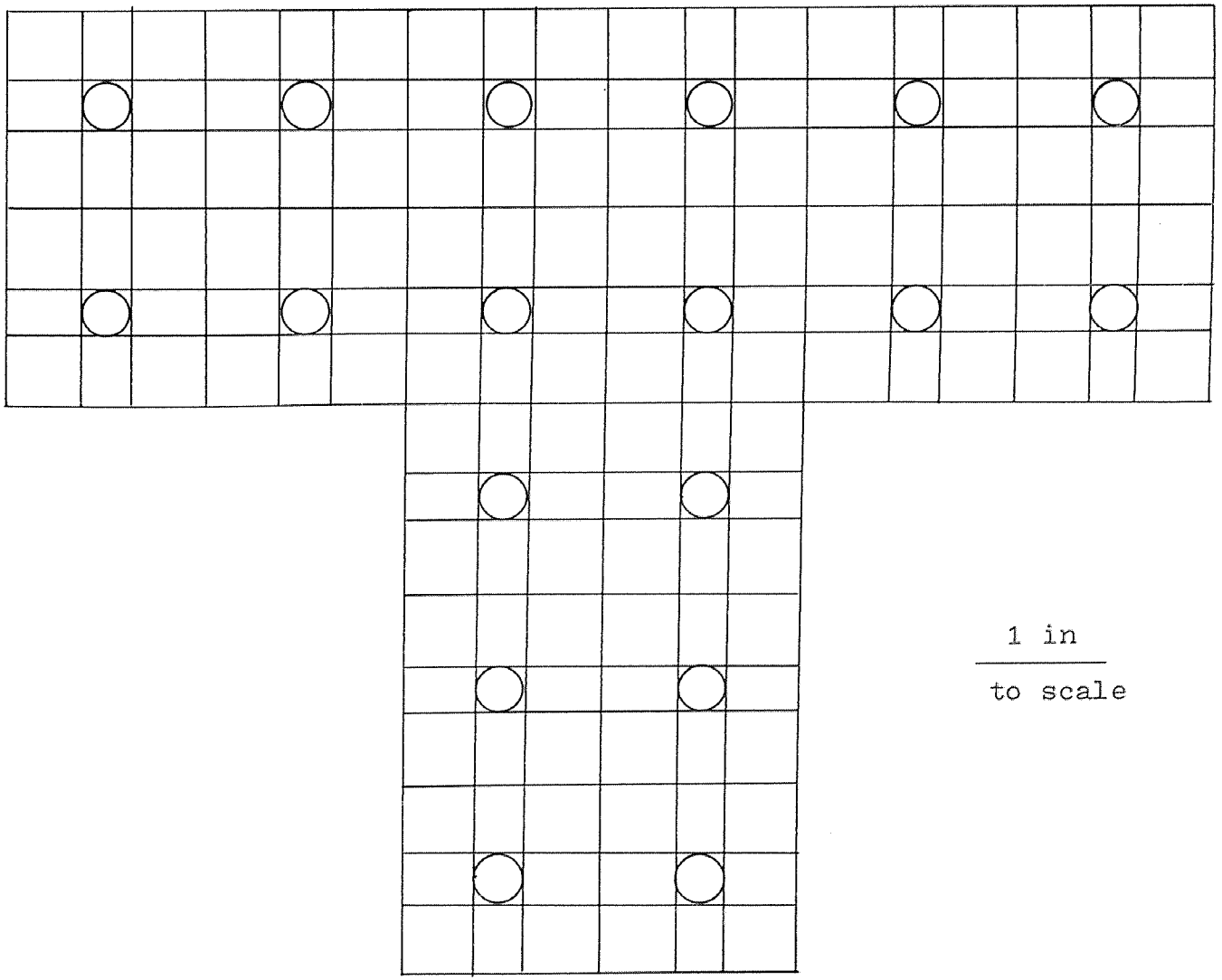

Figure B-1 A finite element mesh of the reinforced concrete tee column

Table B-1 Element coordinates and area for computer program input

Element	Area (in^2)	x-coordinate (in)	y-coordinate (in)
1	0.11	-3.753	-2.002
2	0.11	-2.252	-2.002
3	0.11	-0.751	-2.002
4	0.11	0.751	-2.002
5	0.11	2.252	-2.002
6	0.11	3.753	-2.002
7	0.11	3.753	-0.501
8	0.11	2.252	-0.501
9	0.11	0.751	-0.501
10	0.11	0.751	1.001
11	0.11	0.751	2.502
12	0.11	0.751	4.003
13	0.11	-0.751	4.003
14	0.11	-0.751	2.502
15	0.11	-0.751	1.001
16	0.11	-0.751	-0.501
17	0.11	-2.252	-0.501
18	0.11	-3.753	-0.501
19	0.317	-4.222	-0.032
20	0.211	-4.222	-0.501
21	0.317	-4.222	-0.970
22	0.317	-4.222	-1.533
23	0.211	-4.222	-2.002

Element	Area (in^2)	x-coordinate (in)	y-coordinate (in)
24	0.317	-4.222	-2.471
25	0.211	-3.753	-2.471
26	0.317	-3.284	-2.471
27	0.317	-2.721	-2.471
28	0.211	-2.252	-2.471
29	0.317	-1.783	-2.471
30	0.317	-1.22	-2.471
31	0.211	-0.751	-2.471
32	0.317	-0.282	-2.471
33	0.317	0.282	-2.471
34	0.211	0.751	-2.471
35	0.317	1.22	-2.471
36	0.317	1.783	-2.471
37	0.211	2.252	-2.471
38	0.317	2.721	-2.471
39	0.317	3.284	-2.471
40	0.317	3.753	-2.471
41	0.317	4.222	-2.471
42	0.211	4.222	-2.002
43	0.317	4.222	-1.533
44	0.317	4.222	-0.970
45	0.211	4.222	-0.501
46	0.317	4.222	-0.032

Element	Area (in^2)	x-coordinate (in)	y-coordinate (in)
47	0.211	3.753	-0.032
48	0.317	3.284	-0.032
49	0.317	2.721	-0.032
50	0.211	2.252	-0.032
51	0.317	1.783	-0.032
52	0.317	1.22	-0.032
53	0.317	1.22	-0.032
54	0.211	1.22	1.001
55	0.317	1.22	1.470
56	0.317	1.22	2.033
57	0.211	1.22	2.502
58	0.317	1.22	2.971
59	0.317	1.22	3.534
60	0.211	1.22	4.003
61	0.317	1.22	4.472
62	0.211	0.751	4.472
63	0.317	0.282	4.472
64	0.317	-0.282	4.472
65	0.211	-0.751	4.472
66	0.317	-1.22	4.472
67	0.211	-1.22	4.003
68	0.317	-1.22	3.534
69	0.317	-1.22	2.971

Element	Area (in^2)	x-coordinate (in)	y-coordinate (in)
70	0.211	-1.22	2.502
71	0.317	-1.22	2.033
72	0.317	-1.22	1.470
73	0.211	-1.22	1.001
74	0.317	-1.22	0.532
75	0.317	-1.22	-0.032
76	0.317	-1.783	-0.032
77	0.211	-2.252	-0.032
78	0.317	-2.721	-0.032
79	0.317	-3.284	-0.032
80	0.211	-3.753	-0.032
81	0.211	-3.753	-0.970
82	0.211	-3.753	-1.533
83	0.211	-3.284	-2.002
84	0.211	-2.721	-2.002
85	0.211	-1.783	-2.002
86	0.211	-1.22	-2.002
87	0.211	-0.282	-2.002
88	0.211	0.282	-2.002
89	0.211	1.22	-2.002
90	0.211	1.783	-2.002
91	0.211	2.721	-2.002
92	0.211	3.284	-2.002
93	0.211	3.753	-1.533

Element	Area (in^2)	x-coordinate (in)	y-coordinate (in)
94	0.211	3.753	-0.970
95	0.211	3.284	-0.501
96	0.211	2.721	-0.501
97	0.211	1.783	-0.501
98	0.211	1.22	-0.501
99	0.211	0.751	-0.032
100	0.211	0.751	0.532
101	0.211	0.751	1.470
102	0.211	0.751	2.033
103	0.211	0.751	2.971
104	0.211	0.751	3.534
105	0.211	0.282	4.003
106	0.211	-0.282	4.003
107	0.211	-0.751	3.534
108	0.211	-0.751	2.971
109	0.211	-0.751	2.033
110	0.211	-0.751	1.470
111	0.211	-0.751	0.532
112	0.211	-0.751	-0.032
113	0.211	-1.22	-0.501
114	0.211	-1.783	-0.501
115	0.211	-2.721	-0.501
116	0.211	-3.284	-0.501

Element	Area (in^2)	x-coordinate (in)	y-coordinate (in)
117	0.317	-3.284	-0.970
118	0.317	-3.284	-1.533
119	0.317	-2.721	-1.533
120	0.211	-2.252	-1.533
121	0.317	-1.783	-1.533
122	0.317	-1.22	-1.533
123	0.211	-0.751	-1.533
124	0.317	-0.282	-1.533
125	0.317	0.282	-1.533
126	0.211	0.751	-1.533
127	0.317	1.22	-1.533
128	0.317	1.783	-1.533
129	0.211	2.252	-1.533
130	0.317	2.721	-1.533
131	0.317	3.284	-1.533
132	0.317	3.284	-0.970
133	0.317	2.721	-0.970
134	0.211	2.252	-0.970
135	0.317	1.783	-0.970
136	0.317	1.22	-0.970
137	0.211	0.751	-0.970
138	0.317	0.282	-0.970
139	0.211	0.282	-0.501

Element	Area (in^2)	x-coordinate (in)	y-coordinate (in)
140	0.317	0.282	-0.032
141	0.317	0.282	0.532
142	0.211	0.282	1.001
143	0.317	0.282	1.470
144	0.317	0.282	2.033
145	0.211	0.282	2.502
146	0.317	0.282	2.971
147	0.317	0.282	3.534
148	0.317	-0.282	3.534
149	0.317	-0.282	2.971
150	0.211	-0.282	2.502
151	0.317	-0.282	2.033
152	0.317	-0.282	1.470
153	0.211	-0.282	1.001
154	0.317	-0.282	0.532
155	0.317	-0.282	-0.032
156	0.211	-0.282	-0.501
157	0.317	-0.282	-0.970
158	0.211	-0.751	-0.970
159	0.317	-1.22	-0.970
160	0.317	-1.783	-0.970
161	0.211	-2.252	-0.970
162	0.317	-2.721	-0.970

Selected Bibliography

(1) Au, Tung, " Ultimate strength design of rectangular concrete members subject to unsymmetrical bending ", ACI Journal, Proceedings v.54, February 1958, pp. 657-674

(2) Berwanger, C., " Effect of axial load on the moment-curvature relationship of reinforced concrete members ", Symposium on reinforced concrete columns, ACI, SP-50, 1975, p.263.

(3) Bresler, Boris, " Design criteria for reinforced concrete columns under axial load and biaxial bending ", ACI Journal, Proceedings v.57, November 1960, pp.481-490.

(4) Craemer, Hermann, " Skew bending in concrete computed by plasticity ", ACI Journal, Proceedings v.48, February 1952, pp.516-519.

(5) Cranston, W.B., " Determining the relation between moment, axial load and curvature for structural members ", Technical Report TRA 395, Cement and Concrete Association, London, June 1966.

(6) Farah, A. and Huggins, M.W., " Analysis of reinforced concrete columns subjected to longitudinal load and biaxial bending ", ACI Journal, Proceedings, July 1969, p.569.

(7) Fleming, John F., and Werner, Stuart D., " Design of columns subjected to biaxial bending ", ACI Journal, Proceedings v.62, March 1965, pp.327-342.

(8) Ford, J.G., Chang, D.C. and Breen, J.E., " Behavior of concrete columns under controlled lateral deformation ", Proceedings, ACI, January 1981, p.3.

(9) Furlong, R.W., " Concrete columns under biaxially eccentric thrust ", Proceedings, ACI, October 1979, p.1093.

(10) Furlong, Richard M., " Ultimate strength of square columns under biaxially eccentric loads ", ACI Journal, Proceedings v.57, March 1961, pp.1129-1140.

(11) Gouwens, A.J., " Biaxial bending simplified ", Symposium on reinforced concrete columns, ACI, SP-50, 1975, p.233.

(12) Heimdahl, P.D. and Bianchini, A.C., " Ultimate strength of biaxially eccentrically loaded concrete columns reinforced with high strength steel ", Symposium on reinforced concrete columns, ACI, SP-50, 1975, 93.

(13) Hsu, C.T.T., " Behavior of structural concrete subjected to biaxial flexure and axial compression ", Ph.D. Thesis, McGill University, August 1974.

(14) Chu, K.H., and Pabarcius, A., " Biaxially loaded reinforced concrete columns ", Proceedings, ASCE, v.84, ST8, December 1958, pp.1865-1 to 1865-27.

(15) Marin, J., " Design aids for L-shaped reinforced concrete columns ", Proceedings, ACI, November 1979, p.1197.

(16) Meek, John L., " Ultimate strength of columns with biaxially eccentric loads ", ACI Journal, Proceedings v.60, No.8, August 1963, pp.1053-1064.

(17) Pannell, F.N., " Failure surfaces for members in compression and biaxial bending ", Proceedings, ACI, 1963, p.129.

(18) Ramamurthy, L.N., " Investigation of the ultimate strength of squares and rectangular columns under biaxially eccentric loads ", Symposium on reinforced concrete columns, ACI, SP-13, 1966, p.263.

(19) Wang, C.K. and Solmon, C.G., " Reinforced concrete design ", Harper and Row, New York, 1979.

(20) Winter, G. and Nilson, A.H., " Design of concrete structures ", McGraw-Hill, 1979.